

Effects of the interplay between fermionic interactions and disorders in the nodal-line superconductors

Wen-Hao Bian,¹ Xiao-Zhuo Chu,¹ and Jing Wang^{1,2,*}

¹*Department of Physics, Tianjin University, Tianjin 300072, P.R. China*

²*Tianjin Key Laboratory of Low Dimensional Materials Physics and Preparing Technology, Tianjin University, Tianjin 300072, P.R. China*

(Dated: August 9, 2023)

We carefully study the interplay between short-range fermion-fermion interactions and disorder scatterings beneath the superconducting dome of the noncentrosymmetric nodal-line superconductors. With the application of renormalization group, the energy-dependent coupled flows of all these associated interaction parameters are established after taking into account the potential low-energy physical ingredients including both kinds of fermionic interactions and disorder couplings as well as their competitions on the same footing. Encoding the low-energy information from these entangled evolutions gives rise to several interesting behaviors in the low-energy regime. At the clean limit, fermion-fermion interactions decrease with lowering the energy scales but conversely fermion velocities climb up and approach certain saturated values. This yields a slight decrease or increase in the anisotropy of fermion velocities depending upon their initial ratio. After bringing out four kinds of disorders designated by the random charge (Δ_1), random mass (Δ_2), random axial chemical potential (Δ_3), and spin-orbit scatterers (Δ_4) based on their own unique features, we begin with presenting the distinct low-energy fates of these disorders. For the presence of sole disorder, its strength becomes either relevant ($\Delta_{1,4}$) or irrelevant ($\Delta_{2,3}$) in the low-energy regime. However, the competition for multiple sorts of disorders is capable of qualitatively reshaping the low-energy properties of disorders $\Delta_{2,3,4}$. Besides, it can generate an initially absent disorder as long as two of $\Delta_{1,2,3}$ are present. In addition, the fermion-fermion couplings are insensitive to the presence of disorder Δ_4 but rather substantially modified by Δ_1 , Δ_2 , or Δ_3 , and they evolve toward zero or certain finite nonzero values under the coexistence of distinct disorders. Furthermore, the fermion velocities flow toward certain finite saturated value for the only presence of $\Delta_{2,3}$ and vanish for all other situations. As to their ratio, it acquires a little increase once the disorder is subordinate to fermion-fermion interactions, otherwise keeps some fixed constant.

I. Introduction

Since the superconductivity was discovered in the beginning of the last century, it has been attracting a vast amount of both experimental and theoretical efforts and becoming one of the most important and hottest topics in contemporary condensed matter physics. Principally, conventional superconductors that are well understood by the celebrated BCS theory [1] possess an isotropic s -wave gap so that the gapless fermionic excitations are not allowed in the low-energy regime due to the absence of any nodal points around the Fermi surface [2–4]. In marked comparison, most of the cuprate high-temperature superconductors (HTSCs) can be regarded as effectively (quasi) two-dimensional compounds [5–7]. Particularly, these HTSCs are commonly equipped with a d -wave superconducting gap which allows four gapless nodal points on the Fermi surface. [5, 8–12]. As a result, the gapless fermionic quasiparticles can be always excited even at the lowest-energy limit to participate in potential physical processes and induce a plethora of critical behaviors [5]. Besides these very

nodal-point materials, a number of groups advocated that there are several three-dimensional (3D) compounds including the heavy-fermion superconductors CePtSi₃ [13–15], UCoGe [16, 17] and pnictides superconductors Ba(Fe_{1-x}Co_x)₂As₂ [18, 19], FeSe [20, 21] and (Ba_{1-x}K_x)Fe₂As₂ [22], which share an analogous but revised version of nodal structure with cuprate HTSCs, namely, owning the nodal-line points as illustrated in Fig. 1, and are consequently dubbed the nodal-line superconductors.

Without loss of generality, there at least exist three major ingredients including the dispersion of low-energy excitations as well as fermion-fermion interactions and disorder scatterers, which are expected to play a crucial role in determining the low-energy physical properties involving the ground states, transport quantities, etc. [5, 23–30]. Recently, the significant roles of electronic correlations and their couplings with other physical degrees in pinning down the low-energy fates and underlying phase transitions of fermionic materials have gradually attracted a great attention [31–40]. Additionally, disorder scatterings that are always present in the real compounds have been verified to induce a multitude of singular behaviors in the low-energy regime [23–28, 30, 38, 41–58]. Considering unique topologies of their Fermi surfaces [59–61],

* Corresponding author: jing_wang@tju.edu.cn

the gapless fermionic excitations can always be excited from the nodal lines of nodal-line superconductors. On the one hand, such gapless excitations are naturally interacted with each other [29, 62–64]. On the other hand, they can intimately entangle with disorder scatterings. These accordingly can result in a plethora of unusual but interesting behaviors with lowering the energy scales [29, 38, 62–66]. It is, therefore, imperative to unbiasedly take into account both fermion-fermion interactions and impurities to capture more physical information in the low-energy regime. A question naturally raises how the fermion-fermion interactions and disorders influence the physical behaviors.

Stimulated by these, we within this work endeavor to investigate the effects of interplay between short-range fermion-fermion interactions and disorder scatterings on the low-energy fates in the superconducting dome of nodal-line superconductors. After carrying both attentively analytical and numerical studies, several interesting results are obtained with the help of renormalization group (RG) approach [67–69] that treats all the physical ingredients on the equal footing.

For completeness, four distinct types of disorders are taken into account, which are dubbed the random charge (Δ_1), random mass (Δ_2), random axial chemical potential (Δ_3), and spin-orbit scatterers (Δ_4) as defined in Eq. (11) based on their own unique features [39, 70]. As for the clean limit, we find that the fermionic couplings tend to decrease with lowering the energy scale but instead the fermion velocities designated in Eq. (12) climb up and eventually become saturated attesting to the contributions from fermion-fermion interactions. Besides, the anisotropy of fermion velocities characterized by v_z/v_p alters and obtains a slight decrease or increase for the initial condition $v_{z0}/v_{p0} < 1$ or $v_{z0}/v_{p0} > 1$, respectively.

In comparison, the phenomena are more interesting under the competition between fermion-fermion and disorders interactions. At first, for the presence of sole disorder, we notice that the disorder strength gradually decreases and eventually vanishes with lowering the energy scale ($\Delta_{2,3}$), and becomes relevant and goes toward divergence ($\Delta_{1,4}$), respectively. Such divergence of disorder may turn the system into a disorder-dominated diffusive metallic state [48, 71–76]. As to the presence of multiple sorts of disorders, the disorder Δ_1 strength shares the similar evolution with its sole presence's but rather the fates of other three types of disorders are qualitatively reformulated, with Δ_4 being driven irrelevant and Δ_2 (or Δ_3) being changed from vanishment to divergence. It is also of particular importance to highlight that an additional sort of disorder which is absent initially can be generated due to the interplay of multi-type disorders as long as any two of three sorts of disorders Δ_1 , Δ_2 , and Δ_3 are present at the starting point. In addition, we figure out that, compared to

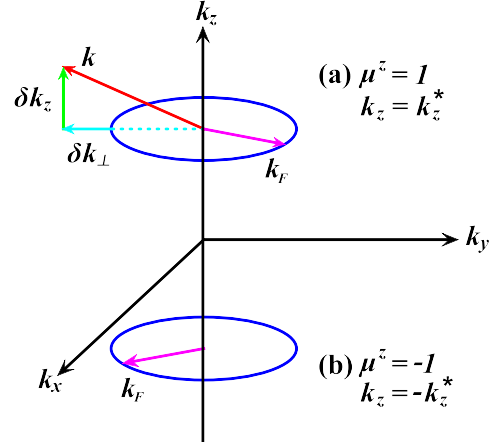


FIG. 1. (Color online) Schematic structure for low-energy nodal-line excitations.

their clean-limit counterparts, the evolutions of fermion-fermion interactions are insusceptible to the sole presence of disorder Δ_4 . In contrast, the single presence of Δ_1 , Δ_2 , or Δ_3 is able to dramatically modify the fates of fermion-fermion interactions and hence make them more significant in the low-energy regime and even divergent at certain critical energy after involving the disorder contributions. However, the furious competition among distinct types of disorders can be harmful to the divergence of fermionic couplings and render them flowing toward zero or certain finite nonzero values. Furthermore, under the competition between fermionic interactions and disorder scatterings, the fermion velocities are prone to evolving toward zero for the sole presence of Δ_1 (or Δ_4) or more than two kinds of disorders but certain saturated value for the single presence of Δ_2 (or Δ_3). As to the ratio v_z/v_p , it nearly remains some fixed value once the fermion-fermion interactions are subordinate to the disorder contribution but instead obtains a little increase while the disorder becomes less and less important, and the fermion-fermion interaction can provide more significant contributions in the low-energy regime.

We organize the rest of this paper as follows. The microscopic model is introduced to establish the effective field theory in Sec. II. Then, Sec. III is followed to carry out the RG analysis and derive the coupled evolution equations of all fermion-fermion interaction parameters and disorder strengths. Then, we within Sec. IV perform a warm-up for the clean limit situation. Thereafter, Sec. V presents the fates of disorder couplings as well as fermion-fermion interactions and fermion velocities. At last, Sec. VI provides a short summary of our main results.

II. Microscopic model and effective action

A. Free microscopic model

We put our focus on the topological nodal-line superconductors that satisfy a common symmetry group $\mathcal{G} = C_{4v} \times \mathcal{T} \times \mathcal{P}$ with \mathcal{T} and \mathcal{P} , respectively, corresponding to the time-reversal and particle-hole symmetries [77], and begin with the following noninteracting Hamiltonian to characterize the low-energy excitations from their nodal-line points [77, 78],

$$H_0 = \sum_{\mathbf{k}} \Psi_{\mathbf{k}}^\dagger [h(\mathbf{k})\tau^z + \Delta(\mathbf{k})\tau^x] \Psi_{\mathbf{k}}, \quad (1)$$

where the four component spinor is designated as $\Psi_{\mathbf{k}}^\dagger = (\chi_{\mathbf{k}}^\dagger, i\sigma^y \chi_{-\mathbf{k}}^T)$ with $\chi_{\mathbf{k}}^\dagger = (c_{\mathbf{k}\uparrow}^*, c_{\mathbf{k}\downarrow}^*)$ [78]. In addition, the Pauli matrices $\tau^{x,y,z}$ and $\sigma^{x,y,z}$ apply to the particle-hole space and spin space, respectively. Furthermore, the normal-state term $h(\mathbf{k})$ and pairing gap function $\Delta(\mathbf{k})$ are expressed as [78–80]

$$h(\mathbf{k}) = \varepsilon(\mathbf{k}) - \mu + \alpha \mathbf{l}(\mathbf{k}) \cdot \boldsymbol{\sigma}, \quad (2)$$

$$\Delta(\mathbf{k}) = \Delta_s + \Delta_t \mathbf{d}(\mathbf{k}) \cdot \boldsymbol{\sigma}, \quad (3)$$

where the spin-orbital coupling is specified by the parameter α in Eq. (2) and the energy dispersion reads

$$\begin{aligned} \varepsilon(\mathbf{k}) &= -2t(\cos k_x + \cos k_y + \cos k_z) \\ &\approx t(k_x^2 + k_y^2 + k_z^2) - 6t, \end{aligned} \quad (4)$$

with the parameter t being the hopping constant. Additionally, the pairing amplitudes Δ_s and Δ_t are assumed to be real and positive due to the \mathcal{T} symmetry of topological nodal-line superconductors [78–80].

It is of particular necessity to bear in mind that the nodal-line points can only be realized while the negative eigenvalue of $\mathbf{l}(\mathbf{k}) \cdot \boldsymbol{\sigma}$ with $-\mathbf{d}(\mathbf{k})$ is taken into account [78]. In addition, one for the sake of simplicity can consider that the spin-orbital and pairing term share the same direction [78, 79],

$$\mathbf{d}(\mathbf{k}) = \mathbf{l}(\mathbf{k}) = (\sin(k_x), \sin(k_y), 0) = \mathbf{k}_\perp. \quad (5)$$

After performing the Taylor expansion neighboring the nodal-line points as displayed in Fig. 1 which consists of two analogous nodal rings dubbed by $\mu^z = 1$ and $\mu^z = -1$, the effective Hamiltonian can be reformulated as [78]

$$H_0 = \int \frac{d^3\mathbf{k}}{(2\pi)^3} \psi_{\mathbf{k}}^\dagger (v_z \delta k_z \Sigma_{03} + v_p \delta k_\perp \Sigma_{01}) \psi_{\mathbf{k}}. \quad (6)$$

Herein, we adopt the transformation $\zeta \delta k_\perp + v_z \delta k_z \rightarrow v_z \delta k_z$ (i.e., $\delta k_z \rightarrow \delta k_z - \zeta \delta k_\perp / v_z$) and introduce two fermion velocities v_z and v_p that are tied to the microscopic parameters k_z^* , m , as well as Δ_t [78]. In addition,

the 4×4 matrix $\Sigma_{\mu\nu}$ is designated as $\Sigma_{\mu\nu} \equiv \sigma_\mu \otimes \tau_\nu$ with $\mu, \nu = 0, 1, 2, 3$. Hereby, the four-component spinor $\psi_{\mathbf{k}}^T = (c_{\mathbf{k}\uparrow}, c_{-\mathbf{k}\uparrow}, c_{\mathbf{k}\downarrow}, c_{-\mathbf{k}\downarrow})$ is nominated to specify the excited nodal fermions surrounding the upper ($\mu^z = 1$) and lower ($\mu^z = -1$) nodal rings in Fig. 1 with k_F serving as the radius of the nodal line. Further, δk_z and $\delta k_\perp^2 = \delta k_x^2 + \delta k_y^2$ designate the transfer momenta of the low-energy fermionic excitations in the k_z direction and $k_x - k_y$ plane around the nodal line, respectively.

B. Fermion-fermion interactions and disorder scatterings

To proceed, we bring out the short-ranged fermion-fermion interactions to characterize the potential role played by the low-energy excitations from nodal lines [32, 33, 45, 70, 78, 81–83],

$$\begin{aligned} S_{\text{ff}} &= \sum_{\mu\nu=0}^3 \lambda_{\mu\nu} \prod_{j=1}^4 \int \frac{d^3\mathbf{k}_j d\omega_j}{(2\pi)^4} \psi_{\mathbf{k}_1, \omega_1}^\dagger \Sigma_{\mu\nu} \psi_{\mathbf{k}_2, \omega_2} \psi_{\mathbf{k}_3, \omega_3}^\dagger \Sigma_{\mu\nu} \psi_{\mathbf{k}_4, \omega_4} \\ &\quad \times \delta(\mathbf{k}_1 + \mathbf{k}_2 + \mathbf{k}_3 - \mathbf{k}_4) \delta(\omega_1 + \omega_2 + \omega_3 - \omega_4), \end{aligned} \quad (7)$$

where the vertex matrices $\Sigma_{\mu\nu} \equiv \sigma_\mu \otimes \tau_\nu$ as aforementioned and $\lambda_{\mu\nu}$ are employed to measure the strengths of fermion-fermion couplings with $\mu, \nu = 0, 1, 2, 3$.

In principle, these 16 kinds of fermion-fermion interactions are not all independent among each other. In order to examine and pick out the independent ones, we resort to the Fierz identity [37, 70, 84]. With the spirit of such an identity, a general interacting term can be expressed as,

$$\begin{aligned} &(\psi^\dagger \mathcal{M} \psi)(\psi^\dagger \mathcal{N} \psi) \\ &= -\frac{1}{16} \sum_{a=1}^{16} \text{Tr}(\mathcal{M} \Gamma^a \mathcal{N} \Gamma^b) (\psi^\dagger \Gamma^b \psi) (\psi^\dagger \Gamma^a \psi), \end{aligned} \quad (8)$$

where \mathcal{M} , \mathcal{N} , and Γ denote certain 4×4 matrices with requiring $(\Gamma^a)^\dagger = \Gamma^a = (\Gamma^a)^{-1}$. This indicates that any sort of interactions appearing in Eq. (7) is allowed to be written by the combinations of parts of these couplings.

To be specific, we hereby following the strategy [37, 70, 84, 85] introduce the interaction vector $\mathcal{V} = \{(\psi^\dagger \Sigma_{00} \psi)^2, (\psi^\dagger \Sigma_{01} \psi)^2, (\psi^\dagger \Sigma_{02} \psi)^2, (\psi^\dagger \Sigma_{03} \psi)^2, (\psi^\dagger \Sigma_{10} \psi)^2, (\psi^\dagger \Sigma_{11} \psi)^2, (\psi^\dagger \Sigma_{12} \psi)^2, (\psi^\dagger \Sigma_{13} \psi)^2, (\psi^\dagger \Sigma_{20} \psi)^2, (\psi^\dagger \Sigma_{21} \psi)^2, (\psi^\dagger \Sigma_{22} \psi)^2, (\psi^\dagger \Sigma_{23} \psi)^2, (\psi^\dagger \Sigma_{30} \psi)^2, (\psi^\dagger \Sigma_{31} \psi)^2, (\psi^\dagger \Sigma_{32} \psi)^2, (\psi^\dagger \Sigma_{33} \psi)^2\}$. After adopting Eq. (8), we are left with $\sum_{j=1}^{16} \frac{1}{4} \mathcal{F}_{ij} \mathcal{V}_j = 0$ where \mathcal{F} takes the form of

$$\mathcal{F} = \begin{pmatrix} 5 & 1 & 1 & 1 & 1 & 1 & 1 & 1 & 1 & 1 & 1 & 1 & 1 & 1 & 1 & 1 \\ 1 & 5 & -1 & -1 & 1 & 1 & -1 & -1 & 1 & 1 & -1 & -1 & 1 & 1 & -1 & -1 \\ 1 & -1 & 5 & -1 & 1 & -1 & 1 & -1 & 1 & -1 & 1 & -1 & 1 & -1 & 1 & -1 \\ 1 & -1 & -1 & 5 & 1 & -1 & -1 & 1 & 1 & -1 & -1 & 1 & 1 & -1 & -1 & 1 \\ 1 & 1 & 1 & 1 & 5 & 1 & 1 & 1 & -1 & -1 & -1 & -1 & 1 & 1 & -1 & -1 \\ 1 & 1 & -1 & -1 & 1 & 5 & -1 & -1 & -1 & -1 & 1 & 1 & -1 & -1 & 1 & 1 \\ 1 & -1 & 1 & -1 & 1 & -1 & 5 & -1 & -1 & -1 & 1 & -1 & 1 & -1 & 1 & -1 \\ 1 & -1 & -1 & 1 & 1 & -1 & -1 & 5 & -1 & 1 & 1 & -1 & -1 & 1 & 1 & -1 \\ 1 & 1 & 1 & -1 & -1 & -1 & -1 & -1 & 5 & 1 & 1 & 1 & -1 & -1 & -1 & -1 \\ 1 & 1 & -1 & -1 & -1 & -1 & 1 & 1 & 1 & 5 & -1 & -1 & -1 & -1 & 1 & 1 \\ 1 & -1 & 1 & -1 & -1 & 1 & -1 & 1 & 1 & -1 & 5 & -1 & -1 & 1 & -1 & 1 \\ 1 & -1 & -1 & 1 & -1 & 1 & -1 & 1 & -1 & -1 & 5 & -1 & 1 & 1 & 1 & -1 \\ 1 & 1 & 1 & 1 & -1 & -1 & -1 & -1 & -1 & -1 & -1 & 5 & 1 & 1 & 1 & 1 \\ 1 & 1 & -1 & -1 & -1 & -1 & 1 & 1 & -1 & -1 & 1 & 1 & 5 & -1 & -1 & -1 \\ 1 & -1 & 1 & -1 & -1 & 1 & -1 & 1 & -1 & 1 & -1 & 1 & 1 & -1 & 5 & -1 \\ 1 & -1 & -1 & 1 & -1 & 1 & 1 & -1 & -1 & 1 & 1 & -1 & 1 & -1 & -1 & 5 \end{pmatrix}$$

With the help of linear algebra, this gives rise to $\text{rankNull}(\mathcal{F}) = 6$ signaling only six independent couplings. Without loss of generality, we hereafter select six representative couplings in Eq. (7) as the effective fermion-fermion interactions and henceforth reformulate the interaction terms into

$$S_{\text{int}} = \sum_{i=1}^6 \lambda_i \prod_{j=1}^4 \int \frac{d^3 \mathbf{k}_j d\omega_j}{(2\pi)^4} \psi_{\mathbf{k}_1, \omega_1}^\dagger \mathcal{M}_i \psi_{\mathbf{k}_2, \omega_2} \psi_{\mathbf{k}_3, \omega_3}^\dagger \mathcal{M}_i \psi_{\mathbf{k}_4, \omega_4} \times \delta(\mathbf{k}_1 + \mathbf{k}_2 + \mathbf{k}_3 - \mathbf{k}_4) \delta(\omega_1 + \omega_2 + \omega_3 - \omega_4), \quad (9)$$

where \mathcal{M}_i corresponds to $\Sigma_{01}, \Sigma_{03}, \Sigma_{23}, \Sigma_{30}, \Sigma_{31},$ and Σ_{32} as well as λ_i represents the associated strengths with i running from 1 to 6.

Besides the fermion-fermion interactions, we also take into account the effects of a quenched, Gaussian white-noise disorder, which obeys the following restrictions [39, 41–43, 86, 87],

$$\langle \mathcal{D}(\mathbf{x}) \rangle = 0, \quad \langle \mathcal{D}(\mathbf{x}) \mathcal{D}(\mathbf{x}') \rangle = \Delta \delta^{(3)}(\mathbf{x} - \mathbf{x}'). \quad (10)$$

Hereby, \mathcal{D} denotes the impurity field, and the parameter Δ serves as the concentration of the impurity. Averaging over the random impurity potential by virtue of so-called replica method [39, 76, 88–90], the fermion-disorder coupling due to disorder scatterings can be written as follows [39, 70]

$$S_{\text{dis}} = \sum_i \Delta_i \int d\mathbf{x} d\tau d\tau' \psi_\alpha^\dagger(\mathbf{x}, \tau) \Gamma_i \psi_\alpha(\mathbf{x}, \tau) \times \psi_\beta^\dagger(\mathbf{x}, \tau') \Gamma_i \psi_\beta(\mathbf{x}, \tau'), \quad (11)$$

where $\Gamma_1 = \sigma_0 \otimes \tau_0$, $\Gamma_2 = \sigma_0 \otimes \tau_2$, $\Gamma_3 = \sigma_0 \otimes \tau_1$, and $\Gamma_{4j} = \sigma_j \otimes \tau_3$ with $j = 1, 2, 3$ characterize the random charge, random mass, random axial chemical potential, and spin-orbit scatters, respectively [39, 70]. In addition, α, β label the replica indices, and Δ_i is adopted to specify the corresponding strength of fermion-impurity coupling.

C. Effective theory

After combining the free model (6) and the short-ranged fermion-fermion interactions (9) in tandem with the disorder scatterings (11), we can obtain our low-energy effective theory

$$S_{\text{eff}} = \int \frac{d^3 \mathbf{k} d\omega}{(2\pi)^4} \psi_{\mathbf{k}, \omega}^\dagger (-i\omega + v_z \delta k_z \Sigma_{03} + v_p \delta k_\perp \Sigma_{01}) \psi_{\mathbf{k}, \omega} + S_{\text{int}} + S_{\text{dis}}. \quad (12)$$

As a consequence, we can extract the free fermion propagator from the free terms

$$G_0(k) = \frac{1}{-i\omega + v_z \delta k_z \Sigma_{03} + v_p \delta k_\perp \Sigma_{01}}. \quad (13)$$

Given the physical degrees of freedom with small momenta can be excited in the low-energy regime, we only put our focus on the limit $|\delta \mathbf{k}| \ll k_F$ and adopt the following approximation [78–80]

$$\int \frac{d^3 \mathbf{k} d\omega}{(2\pi)^4} \approx \int \frac{d\delta k_z}{2\pi} \int_{k_F} \frac{d\delta k_\perp}{2\pi} \int \frac{d\theta_{\mathbf{k}}}{2\pi} \int \frac{d\omega}{2\pi}, \quad (14)$$

where the radius of nodal ring k_F is schematically presented in Fig. 1.

Afterwards, we consider the effective action (12) as our starting point and are going to derive the coupled RG evolutions of all related parameters appearing in Eq. (12) after involving the intimate relations between fermion-fermion interactions and disorder scatterings, and then examine their consequences on the low-energy physical behaviors in the looming sections.

III. RG analysis of fermion-fermion interactions and disorder strengths

On the basis of Wilsonian momentum-shell RG formalism [67–69], the energy-dependent interaction parameters in the effective action (12) that carry the low-energy information can be established. To this end, we are required to integrate out the fast modes of fields within the momentum shell $b\Lambda < k < \Lambda$, where Λ denotes the energy scale, and the variable parameter b is written as $b = e^{-l}$ with the running energy scale $l > 0$ describing the changes of energy scales [32, 33, 43–45, 69, 91–98]. For convenience, it is helpful to rescale the momenta and energy by Λ_0 that is associated with the lattice constant, i.e., $k \rightarrow k/\Lambda_0$ and $\omega \rightarrow \omega = \omega/\Lambda_0$.

Following the spirit of RG approach [67–69], we subsequently consider the free term of effective theory as an initial fixed point that is invariant under the RG transformation. As a consequence, the RG rescaling transformations of momenta, energy, and fermionic fields, which are employed to connect continuous steps of RG processes, can be derived as follows [43, 69, 91, 93, 95, 99]

$$\omega \rightarrow \omega e^{-l}, \quad (15)$$

$$\delta k_z \rightarrow \delta k_z e^{-l}, \quad (16)$$

$$\delta k_\perp \rightarrow \delta k_\perp e^{-l}, \quad (17)$$

$$\psi_{\mathbf{k}, \omega} \rightarrow \psi_{\mathbf{k}, \omega} e^{\frac{1}{2} \int_0^l dl (4 - \eta_f)}. \quad (18)$$

Hereby, the parameter η_f serves as the anomalous fermion dimension and it collects the intimate contributions from one-loop corrections due to the interplay between fermion-fermion interactions and impurities. As presented in Appendix A, the fermionic self-energy receives nontrivial corrections in the presence of fermion-disorder interplay, which are explicitly provided in Eq. (A1). Combining the RG rescalings (15)-(18) and the free fixed point gives rise to

$$\eta_f = \mathcal{C}_2(\Delta_1 + \Delta_2 + \Delta_3 + \Delta_{41} + \Delta_{42} + \Delta_{43}). \quad (19)$$

With these in hand, we are able to dwell on the RG equations of all interaction parameters appearing in Eq. (12). After long but straightforwardly algebraic calculations, all the one-loop corrections are obtained and presented in Eqs. (A2)-(A13) of Appendix A, which con-

tain the interplay between fermion-fermion interactions and disorder scatterings. Afterwards, adopting these one-loop corrections and paralleling the analogous procedures of RG analysis [43, 69, 91–93, 95] with the help of rescaling transformations (15)-(18) yield the coupled RG flow equations of all coupling parameters,

$$\frac{dv_z}{dt} = [4\mathcal{C}_1\lambda_2 - \mathcal{C}_2(\Delta_1 + \Delta_2 + \Delta_3 + \Delta_{41} + \Delta_{42} + \Delta_{43})]v_z, \quad (20)$$

$$\frac{dv_p}{dt} = [4\mathcal{C}_1\lambda_1 - \mathcal{C}_2(\Delta_1 + \Delta_2 + \Delta_3 + \Delta_{41} + \Delta_{42} + \Delta_{43})]v_p, \quad (21)$$

$$\begin{aligned} \frac{d\lambda_1}{dt} = & 2\lambda_1 \left[-\frac{1}{2} + \mathcal{C}_3(-3\lambda_1 - 2\lambda_2 - \lambda_3 + \lambda_4 + \lambda_5 - \lambda_6) + \mathcal{C}_7(\Delta_1 - \Delta_2 - 7\Delta_3 - \Delta_{41} - \Delta_{42} - \Delta_{43}) \right. \\ & \left. - \mathcal{C}_2(\Delta_1 + \Delta_2 + \Delta_3 + \Delta_{41} + \Delta_{42} + \Delta_{43}) \right], \end{aligned} \quad (22)$$

$$\begin{aligned} \frac{d\lambda_2}{dt} = & 2\lambda_2 \left[-\frac{1}{2} + \mathcal{C}_4(-2\lambda_1 - 3\lambda_2 + \lambda_3 + \lambda_4 - \lambda_5 - \lambda_6) + \mathcal{C}_7(-\Delta_1 + \Delta_2 + \Delta_3 - \Delta_{41} - \Delta_{42} - \Delta_{43}) \right. \\ & \left. - \mathcal{C}_2(\Delta_1 + \Delta_2 + \Delta_3 + \Delta_{41} + \Delta_{42} + \Delta_{43}) \right], \end{aligned} \quad (23)$$

$$\begin{aligned} \frac{d\lambda_3}{dt} = & 2\lambda_3 \left[-\frac{1}{2} + \mathcal{C}_4(-2\lambda_1 + \lambda_2 - 3\lambda_3 - \lambda_4 + \lambda_5 + \lambda_6) + \mathcal{C}_7(-\Delta_1 + \Delta_2 + \Delta_3 + \Delta_{41} + 7\Delta_{42} + \Delta_{43}) \right. \\ & \left. - \mathcal{C}_2(\Delta_1 + \Delta_2 + \Delta_3 + \Delta_{41} + \Delta_{42} + \Delta_{43}) \right] - 4\mathcal{C}_6\lambda_5\Delta_{41}, \end{aligned} \quad (24)$$

$$\frac{d\lambda_4}{dt} = \lambda_4[-1 - 4\mathcal{C}_2(\Delta_{41} + \Delta_{42})] - 4\mathcal{C}_5(\lambda_5\Delta_2 + \lambda_6\Delta_3) - 2\lambda_6(\mathcal{C}_4\lambda_2 + \mathcal{C}_3\lambda_1), \quad (25)$$

$$\begin{aligned} \frac{d\lambda_5}{dt} = & 2\lambda_5 \left[-\frac{1}{2} + \mathcal{C}_3(\lambda_1 - 2\lambda_2 + \lambda_3 + \lambda_4 - 3\lambda_5 - \lambda_6) + \mathcal{C}_7(\Delta_1 - \Delta_2 + \Delta_3 + \Delta_{41} + \Delta_{42} - \Delta_{43}) \right. \\ & \left. - \mathcal{C}_2(\Delta_1 + \Delta_2 + \Delta_3 + \Delta_{41} + \Delta_{42} + \Delta_{43}) \right] + 2\mathcal{C}_1\lambda_2\lambda_6 - 4(\mathcal{C}_6\lambda_3\Delta_{41} + \mathcal{C}_5\lambda_4\Delta_2 + \mathcal{C}_5\lambda_6\Delta_1), \end{aligned} \quad (26)$$

$$\begin{aligned} \frac{d\lambda_6}{dt} = & 2\lambda_6 \left[-\frac{1}{2} + \mathcal{C}_1(-\lambda_1 - \lambda_2 + \lambda_3 + \lambda_4 - \lambda_5 - 3\lambda_6) - (\mathcal{C}_3\lambda_2 + \mathcal{C}_4\lambda_1) - 2\mathcal{C}_2(\Delta_1 + \Delta_2 + \Delta_{41} + \Delta_{42}) \right] \\ & + 2\mathcal{C}_1\lambda_2\lambda_5 - 4\mathcal{C}_5(\lambda_4\Delta_3 + \lambda_5\Delta_1), \end{aligned} \quad (27)$$

$$\frac{d\Delta_1}{dt} = 2\mathcal{C}_2\Delta_1(\Delta_1 + \Delta_2 + \Delta_3 + \Delta_{41} + \Delta_{42} + \Delta_{43}) + 8\mathcal{C}_5\Delta_2\Delta_3, \quad (28)$$

$$\frac{d\Delta_2}{dt} = \Delta_2 \left[2\mathcal{C}_2(-3\Delta_1 - 3\Delta_2 + \Delta_3 + \Delta_{41} + \Delta_{42} + \Delta_{43}) + \mathcal{C}_1(\lambda_1 + \lambda_2 + \lambda_3 - \lambda_4 + \lambda_5 - \lambda_6) \right] + 8\mathcal{C}_5\Delta_1\Delta_3, \quad (29)$$

$$\begin{aligned} \frac{d\Delta_3}{dt} = & \Delta_3 \left[4\mathcal{C}_7(\Delta_1 - \Delta_2 + \Delta_3 - \Delta_{41} - \Delta_{42} - \Delta_{43}) - 2\mathcal{C}_2(\Delta_1 + \Delta_2 + \Delta_3 + \Delta_{41} + \Delta_{42} + \Delta_{43}) \right. \\ & \left. + \mathcal{C}_3(-\lambda_1 + \lambda_2 + \lambda_3 - \lambda_4 - \lambda_5 + \lambda_6) \right] + 8\mathcal{C}_5\Delta_1\Delta_2, \end{aligned} \quad (30)$$

$$\begin{aligned} \frac{d\Delta_{41}}{dt} = & \Delta_{41} \left[4\mathcal{C}_7(-\Delta_1 + \Delta_2 + \Delta_3 - \Delta_{41} + \Delta_{42} + \Delta_{43}) - 2\mathcal{C}_2(\Delta_1 + \Delta_2 + \Delta_3 + \Delta_{41} + \Delta_{42} + \Delta_{43}) \right. \\ & \left. + \mathcal{C}_4(\lambda_1 - \lambda_2 + \lambda_3 + \lambda_4 - \lambda_5 - \lambda_6) \right] + 8\mathcal{C}_5\Delta_{42}\Delta_{43}, \end{aligned} \quad (31)$$

$$\begin{aligned} \frac{d\Delta_{42}}{dt} = & \Delta_{42} \left[4\mathcal{C}_7(-\Delta_1 + \Delta_2 + \Delta_3 + \Delta_{41} - \Delta_{42} + \Delta_{43}) - 2\mathcal{C}_2(\Delta_1 + \Delta_2 + \Delta_3 + \Delta_{41} + \Delta_{42} + \Delta_{43}) \right. \\ & \left. + \mathcal{C}_4(\lambda_1 - \lambda_2 - \lambda_3 + \lambda_4 - \lambda_5 - \lambda_6) \right] + 8\mathcal{C}_5\Delta_{41}\Delta_{43}, \end{aligned} \quad (32)$$

$$\begin{aligned} \frac{d\Delta_{43}}{dt} = & \Delta_{43} \left[4\mathcal{C}_7(-\Delta_1 + \Delta_2 + \Delta_3 + \Delta_{41} + \Delta_{42} - \Delta_{43}) - 2\mathcal{C}_2(\Delta_1 + \Delta_2 + \Delta_3 + \Delta_{41} + \Delta_{42} + \Delta_{43}) \right. \\ & \left. + \mathcal{C}_4(\lambda_1 - \lambda_2 + \lambda_3 - \lambda_4 + \lambda_5 + \lambda_6) \right] + 8\mathcal{C}_5\Delta_{41}\Delta_{42}, \end{aligned} \quad (33)$$

where the coefficients \mathcal{C}_i with $i = 1 - 7$ are nominated

as follows

$$\mathcal{C}_1 \equiv \frac{1}{(2\pi)^3} \int_0^\pi d\theta \frac{\pi}{(v_z^2 \sin^2 \theta + v_p^2 \cos^2 \theta)^{1/2}}, \quad (34)$$

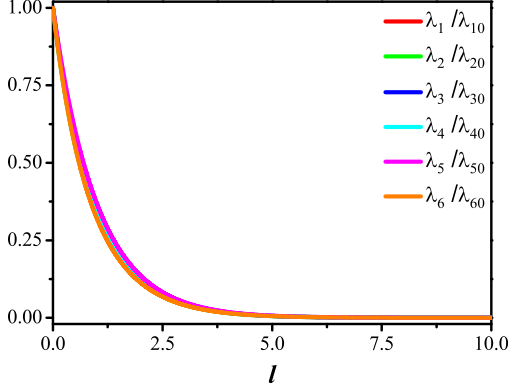


FIG. 2. (Color online) Energy-dependent evolutions of fermion-fermion interaction with $v_{z0}/v_{p0} = 0.1$ and $\lambda_0 = 10^{-3}$ (the qualitative results are insensitive to the initial values of interaction parameters).

$$\mathcal{C}_2 \equiv \frac{1}{(2\pi)^3} \int_0^\pi d\theta \frac{2\pi}{v_z^2 \sin^2 \theta + v_p^2 \cos^2 \theta}, \quad (35)$$

$$\mathcal{C}_3 \equiv \frac{1}{(2\pi)^3} \int_0^\pi d\theta \frac{\pi v_z^2 \sin^2 \theta}{(v_z^2 \sin^2 \theta + v_p^2 \cos^2 \theta)^{3/2}}, \quad (36)$$

$$\mathcal{C}_4 \equiv \frac{1}{(2\pi)^3} \int_0^\pi d\theta \frac{\pi v_p^2 \cos^2 \theta}{(v_z^2 \sin^2 \theta + v_p^2 \cos^2 \theta)^{3/2}}, \quad (37)$$

$$\mathcal{C}_5 \equiv \frac{1}{(2\pi)^3} \int_0^\pi d\theta \frac{4\pi v_z^2 \sin^2 \theta}{(v_z^2 \sin^2 \theta + v_p^2 \cos^2 \theta)^2}, \quad (38)$$

$$\mathcal{C}_6 \equiv \frac{1}{(2\pi)^3} \int_0^\pi d\theta \frac{4\pi v_p^2 \cos^2 \theta}{(v_z^2 \sin^2 \theta + v_p^2 \cos^2 \theta)^2}, \quad (39)$$

$$\mathcal{C}_7 \equiv \frac{1}{(2\pi)^3} \int_0^\pi d\theta \frac{2\pi(v_p^2 \cos^2 \theta - v_z^2 \sin^2 \theta)}{(v_z^2 \sin^2 \theta + v_p^2 \cos^2 \theta)^2}. \quad (40)$$

In this sense, these above entangled evolutions of interaction parameters (20)-(33) bear out that the fermion-fermion interactions as well as fermion-disorder couplings are pertinently coupled and mutually intertwined with each other upon varying of the energy scales. In particular, the fermion velocities including v_z and v_p are also manifestly involved into the coupled equations. Under this circumstance, such energy-dependent couplings can play a direct or indirect role in essentially pinning down the low-energy fates of fermion velocities and interaction parameters. Specifically, we will endeavor to address the clean limit situation in next section IV and defer the disorder effects to Sec. V.

IV. Clean limit

Before moving to the interplay between fermion-fermion interactions and disorder scatterings, we within

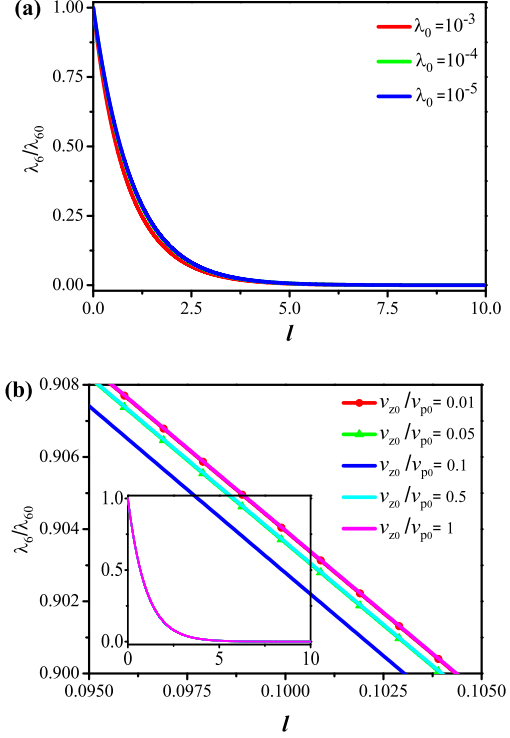


FIG. 3. (Color online) Energy-dependent evolutions of fermion-fermion interaction λ_6/λ_{60} for (a) $v_{z0}/v_{p0} = 0.1$ and distinct values of λ_0 , and (b) $\lambda_0 = 10^{-4}$ and distinct values of anisotropy v_{z0}/v_{p0} (the qualitative results are insensitive to the initial values of interaction parameters).

this section perform a warm-up for the clean limit situation and compare with its disorder counterpart in next section V. Concretely, we primarily account for the consequences of fermion-fermion interactions on the fermion velocities in the absence of disorders.

A. Fates of fermion-fermion interactions

After carrying out the numerical analysis of the energy-dependent coupled RG equations in the absence of disorders, we realize from Fig. 2 for certain representative initial conditions that all of fermion-fermion interactions quickly decrease as the energy scale is lowered and go toward zero at the lowest-energy limit.

Although the starting conditions do not alter the basic fates of fermion-fermion interactions, they can quantitatively modify the energy-dependent behaviors as shown in Fig. 3 for λ_6 as an instance, which shares the similar results with the other five types of interaction couplings. On the one hand, we find that Fig. 3(a) with $v_{z0}/v_{p0} = 0.1$ displays that the fermionic strength decreases a little quickly with the increase in initial

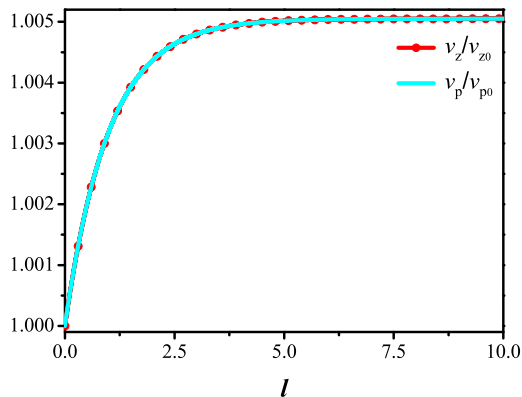


FIG. 4. (Color online) Energy-dependent evolutions of fermion velocities for the isotropic case (v_{z0}/v_{p0}) with $\lambda_0 = 10^{-4}$ (the qualitative results are insensitive to the initial values of interaction parameters).

strength of fermion-fermion interactions. On the other hand, in order to examine the role of initial ratio of fermion velocities in fermionic couplings, we select several representative groups of initial conditions that are distinguished with varying the anisotropy of fermion velocities characterized by v_{z0}/v_{p0} . The related results are displayed in Fig. 3(b). This apparently suggests that the fermion-fermion couplings are insensitive to the anisotropy of fermion velocities, which only slightly impact their values during the intermediate stage with an optimal anisotropy at $v_{z0}/v_{p0} \approx 0.1$ for the decrease in parameters.

On the basis of above analysis, we figure out that these fermion-fermion interactions are irrelevant at the clean limit in the language of RG framework [32, 33, 43–45, 69, 91–97]. Despite their decrease with lowering the energy scale, they still bring interesting corrections to fermion velocities, which are two of particular importance quantities in our effective theory. In addition, it is noteworthy that the irrelevant fates of fermionic interactions at the clean limit would be qualitatively changed under the influence of disorder scatterings, which will be carefully presented in Sec. V.

B. Evolutions of fermion velocities

The two fermion velocities v_z and v_p in our model (12) are of close relevance to the low-energy properties. Accordingly, one needs to study their energy-dependent evolutions that are determined by the coupled RG equations in Sec. III. We hereby endeavor to unveil their low-energy properties at the clean limit. With the help of numerical calculations for the energy-dependent coupled RG equations in the absence of disorders, we provide the

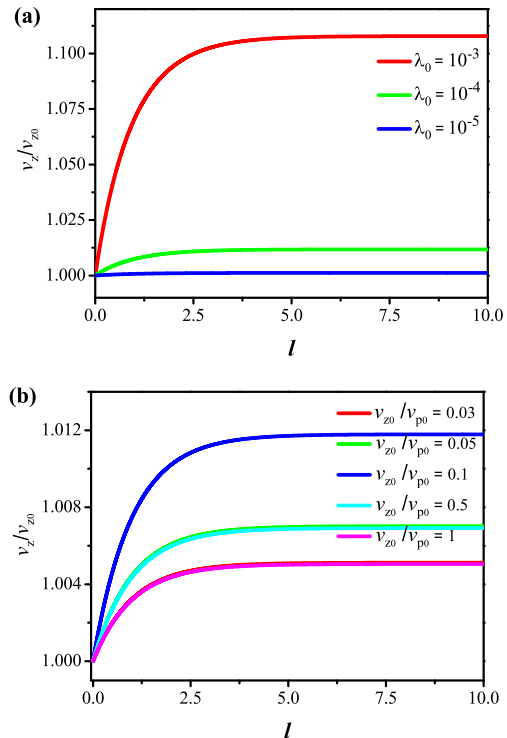


FIG. 5. (Color online) Energy-dependent evolutions of v_z/v_{z0} under: (a) different values of initial fermion-fermion couplings with $v_{z0}/v_{p0} = 0.1$, and (b) different values initial of anisotropy v_{z0}/v_{p0} with $\lambda_0 = 10^{-4}$ (the qualitative results are insensitive to the initial values of interaction parameters).

key energy-dependent tendencies of v_z and v_p as well as v_z/v_p in Figs. 4-6.

Learning from these results, we realize that the fermion-fermion interactions and their effects heavily hinge upon the initial value of anisotropy of fermion velocities. With respect to the initial isotropic fermion velocities (v_{z0}/v_{p0}) shown in Fig. 4, we find that both v_z and v_p gain a slight increase and then be saturated in the sufficiently low-energy scale. In such a circumstance, the ratio of fermion velocities with $v_z/v_p = 1$ is robust against the fermion-fermion interactions with $\lambda_0 = 10^{-4}$ for instance and the basic results are independent of initial values of fermion-fermion couplings. As to the situation with an initial anisotropy of fermion velocities, Fig. 5 and Fig. 6 show that fermion velocities exhibit more interesting behaviors with variations of the fermion-fermion interactions and the ratio of fermion velocities, respectively. Along with Fig. 5(a), we find that v_z climbs up quickly and arrives at a certain constant with lowering the energy scale, which obtains much more increase compared to its isotropic counterpart. Particularly, its saturated value is lifted and ends

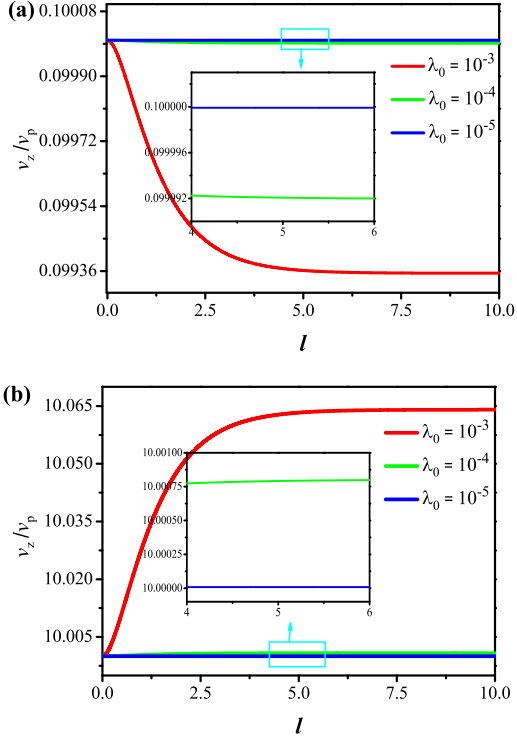


FIG. 6. (Color online) Energy-dependent evolutions of v_z/v_p under different values of initial fermion-fermion couplings with (a) $v_{z0}/v_{p0} = 0.1$ and (b) $v_{z0}/v_{p0} = 10$ (the qualitative results are insensitive to the initial values of interaction parameters).

with some bigger values due to tuning up the starting strengths of fermion-fermion interactions. Additionally, the fermion velocity also depends upon the anisotropy of velocities and aforementioned in Sec. IV A v_z gains the biggest enhancement with an optimal anisotropy at $v_{z0}/v_{p0} \approx 0.1$ as delineated in Fig. 5(b). In comparison, we realize that v_p does not receive the same contribution from fermionic interactions, indicating the change of the initial ratio of v_z and v_p , i.e., initial anisotropy of fermion velocities. To be concrete, it increases a little more than v_z at $v_{z0}/v_{p0} < 1$. As a consequence, v_z/v_p decreases with lowering the energy scales and the increase in the fermionic coupling makes the ratio smaller as displayed in Fig. 6(a). On the contrary, as the velocity v_p receives a little less corrections by lowering the energy scales, we figure out that the ratio of fermion velocities v_z/v_p shown in Fig. 6(b) is driven up at $v_{z0}/v_{p0} > 1$ and goes toward bigger values with increasing the initial fermion-fermion couplings.

To recapitulate, both fermion velocities v_z and v_p are increased as the energy scale is lowered in the absence of disorder scatterings. However, the fate of their ratio v_z/v_p in the low-energy regime is of close association

with its initial condition, which can either fall down at $v_{z0}/v_{p0} < 1$ or climb up at $v_{z0}/v_{p0} > 1$. Although the fermion-fermion interactions are irrelevant and cannot change the basic results, they are able to provide quantitative corrections to the fermion velocities and their ratio in the low-energy regime.

V. Consequences of disorder effects

After addressing the clean-limit situation in the previous section, we hereby endeavor to investigate the effects of disorder scatterings, which are always present in the realistic systems and expected to play an essential role in the low-energy properties of fermionic systems [23–30, 41–56]. With switching on the disorders, on the one hand, the disorder strengths Δ_i with $i = 1 - 4$ introduced in Eq. (11) are forced to interact with each other and fight for their low-energy fates under the ferocious competitions among themselves. On the other hand, they are able to provide considerable influences to the energy-dependent behaviors of both fermion-fermion interactions and fermion velocities by virtue of participating in the entangled RG flows (20)-(33). Afterwards, we are going to address these interesting items one by one in the rest of this section.

A. Low-energy properties of disorder strengths

At the outset, we would like to put our focus on the low-energy behaviors of disorder strengths in that one will figure out later in Sec. VB and Sec. VC that the disorder scatterings can be considered as the impulse or catalyst to trigger a plethora of unusual but interesting behaviors with lowering the energy scales. For the sake of completeness, both the presence of the single type of disorder and multi-type disorders would be carefully delivered as follows.

1. Certain sole type of disorder

Let us begin with the situation of a single sort of disorder. Under such a circumstance, there exists only one equation of disorder strength that survives in the coupled equations (20)-(33). Carrying out the numerical calculations indicates that four kinds of disorders fall into two totally different fates at the lowest-energy limit once one of them inheres alone. Learning from Fig. 7, it is worth pointing out that either the disorder Δ_1 or Δ_4 (as the three components Δ_{4i} with $i = 1, 2, 3$ share with the similar conclusion, we from now on utilize Δ_4 to represent Δ_{4i}) increases upon lowering the energy scale and eventually goes toward diverging at certain critical energy denoted by $l = l_c$. On the contrary, Fig. 8 for

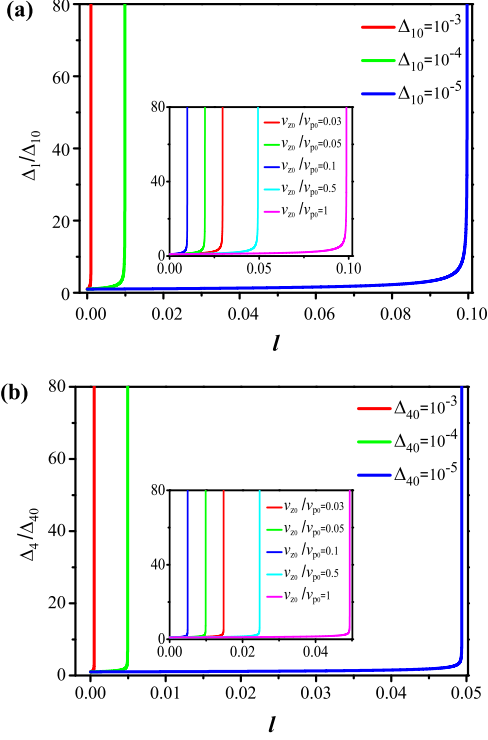


FIG. 7. (Color online) Energy-dependent evolutions of disorder strengths under several representative values of initial strengths at $v_{z0}/v_{p0} = 0.1$ for (a) Δ_1/Δ_{10} with $\lambda_0 = 10^{-3}$ and (b) Δ_4/Δ_{40} with $\lambda_0 = 10^{-4}$. Insets: the evolutions for different values of initial anisotropy v_{z0}/v_{p0} (the qualitative results are insensitive to the initial values of interaction parameters).

the sole presence of Δ_2 or Δ_3 displays that the disorder strength prefers to gradually decrease and finally vanishes at the lowest-energy limit.

As to the presence of disorder Δ_1 or Δ_4 which is prone to divergence as the energy scale is lower enough, we realize that both the starting disorder strengths and initial anisotropy of fermion velocities can be capable of providing considerable impacts on their energy-dependent evolutions and the very critical energy scale at which the instability is triggered. To be specific, one reading from Fig. 7 would manifestly figure out that either the initial value of Δ_1 or Δ_4 is favorable to increase the disorder strength with reducing the energy scale. This accordingly causes the disorder strength divergences at certain smaller l_c indicating of a higher critical energy scale. Compared to the beginning values of disorder strengths, the fermion velocities play a more subtle role in the behaviors of disorders. While the anisotropy of fermion velocities is strong with v_{z0}/v_{p0} taking a comparatively big or small value, it is somewhat harmful to the enhancement of disorder strength as clearly shown in Fig. 7. In contrast, one can learn from Fig. 7 that

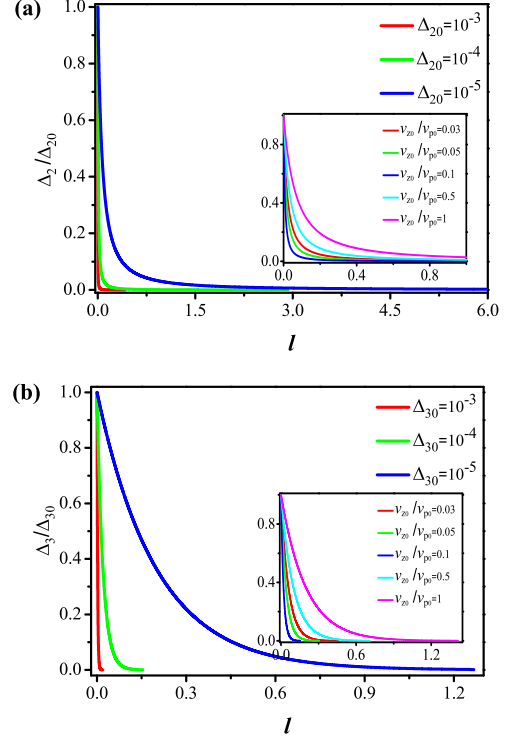


FIG. 8. (Color online) Energy-dependent evolutions of disorder strengths under several representative values of initial strengths at $v_{z0}/v_{p0} = 0.1$ for (a) Δ_2/Δ_{20} with $\lambda_0 = 10^{-3}$ and (b) Δ_3/Δ_{30} with $\lambda_0 = 10^{-4}$. Insets: the evolutions for different values of initial anisotropy v_{z0}/v_{p0} (the qualitative results are insensitive to the initial values of interaction parameters).

a moderate anisotropy is helpful to the increase in disorder strength. The optimal anisotropy is reached at $v_{z0}/v_{p0} \approx 0.1$, which gives rise to a much smaller l_c . With respect to the other two sorts of disorders Δ_2 and Δ_3 , we notice that they exhibit totally different tendencies. Fig. 8 suggests that either Δ_2 or Δ_3 falls off much more rapidly and quickly flows toward zero as long as their initial values are tuned up. Regarding the role played by the anisotropy of fermion velocities, one can readily draw a conclusion from Fig. 8 that the disorder strengths for the sole presence of Δ_2 or Δ_3 climb down more quickly with an intermediate anisotropy than its counterpart equipped with a relatively strong anisotropy. What is more, we examine and realize that the critical energy scale represented by l_c is insusceptible to the initial values of fermion-fermion interactions. Notwithstanding sharing with the same energy-dependent tendencies, $\Delta_{1,4}$ or $\Delta_{2,3}$ still exhibit interesting distinctions between them. Under the same initial conditions with lowering the energy scales, one can obviously learn from Fig. 9 that the disorder strength Δ_4 compared to Δ_1 flows toward divergence

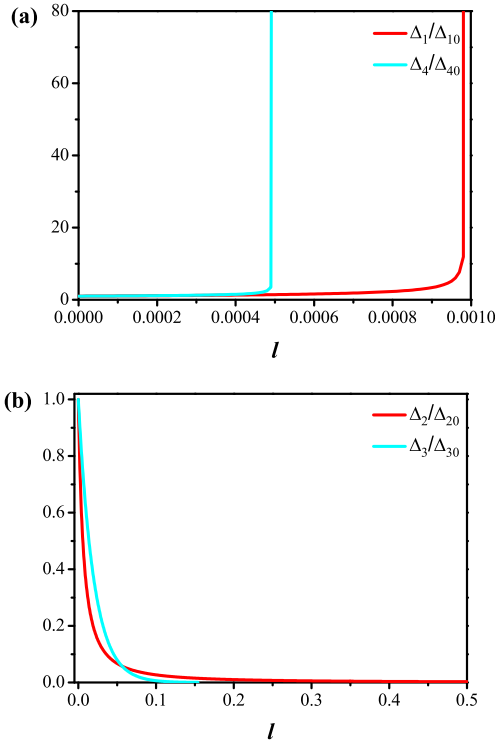


FIG. 9. (Color online) Evolution comparisons with lowering energy scales at $v_{z0}/v_{p0} = 0.1$ and $\lambda_0 = 10^{-4}$ for (a) Δ_1/Δ_{10} and Δ_4/Δ_{40} with $\Delta_{10} = \Delta_{40} = 10^{-3}$, as well as (b) Δ_2/Δ_{20} and Δ_3/Δ_{30} with $\Delta_{20} = \Delta_{30} = 10^{-4}$ (the qualitative results are insensitive to the initial values of interaction parameters).

at some higher energy scale associated with a smaller l_c . Meanwhile, in contrast with Δ_3 , the disorder Δ_2 is a little difficult to be decreased and driven to zero at a much lower energy scale. In other words, the disorder Δ_4 is more relevant but instead Δ_3 becomes more irrelevant in the low-energy regime. Although the numerical results are evaluated on the basis of several representative initial parameters of our theory, we would like to emphasize that the basic conclusions are unsusceptible to their concrete values. Hence, we from now on would not highlight this issue unless it is necessary.

2. Multiple types of disorders

Subsequently, we move to the situations for the simultaneous presence of more than one sort of disorders in which the related equations of disorder strengths (20)-(33) are accompanied. After performing the numerical analysis, we are left with a number of interesting results that are addressed as follows.

First of all, we highlight that the interplay of multi-

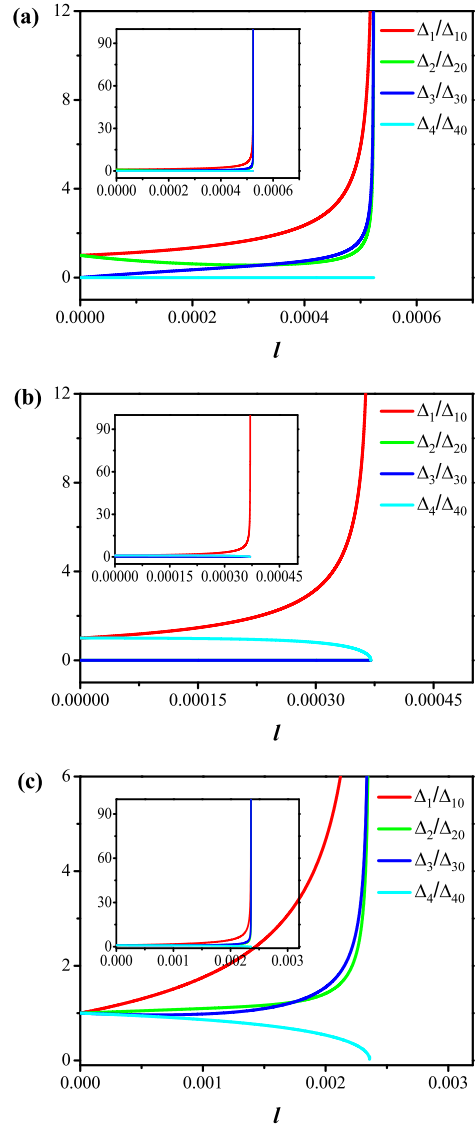


FIG. 10. (Color online) Energy-dependent evolutions of disorder strengths at $v_{z0}/v_{p0} = 0.1$ and $\lambda_0 = 10^{-3}$ for the presence of (a) Δ_1 and Δ_2 with $\Delta_{10} = \Delta_{20} = 10^{-3}$ at the beginning which cause the generation of the Δ_3 , (b) Δ_1 and Δ_4 (its three components are nearly overlapped and hence only of them is presented) cannot induce any type of disorder, and (c) all sorts of disorders with $\Delta_{10} = \Delta_{20} = \Delta_{30} = \Delta_{40} = 10^{-4}$ (the qualitative results are insensitive to the initial values of interaction parameters).

type disorders can generate an additional sort of disorder that is out of the disorders appearing initially. In other words, a new type of disorder without initial strength would receive a finite disorder strength attesting to the evolutions of the coupled equations of disorders. It is then convenient to nominate such phenomenon as the dynamical-generated disorder for fur-

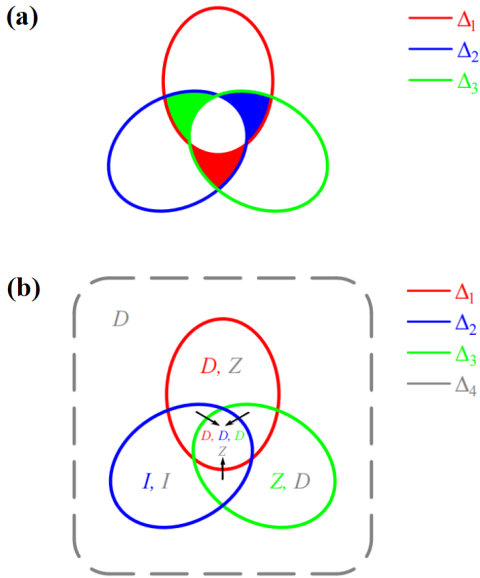


FIG. 11. (Color online) Schematic presentations for the behaviors of distinct kinds of disorders with the regions circled by the red, blue, green, and gray curves denoting the presence of $\Delta_{1,2,3,4}$ at the beginning, respectively. (a) Dynamical-generated disorders: the single presence of disorders $\Delta_{1,2,3}$ cannot develop another type of disorder but instead any two of them are able to induce the third one as labeled by red, blue and green regions (the basic results are insensitive to Δ_4 which hence is not shown). (b) Fates of disorders: the disorder strength for the sole presence of $\Delta_{1,4}$ flows divergently and conversely $\Delta_{2,3}$ goes toward zero. In comparison, they are capable of going either divergently or evolve toward zero as well as hardly changing their initial values (Here D , Z and I equipped with the colors to be associated with different kinds of disorders correspond to being divergent, going toward zero, and approaching the initial values, respectively).

ther discussions. We have examined that these basic conclusions are robust against the starting values of fermion-fermion interactions, which, therefore, in principle are rooted in the intimate competition among distinct types of disorders. To be concrete, certain dynamical-generated disorder is always realized as long as two of disorders Δ_1 , Δ_2 , and Δ_3 are present at the starting point. Taking the presence of disorders Δ_1 and Δ_2 for an instance, Fig. 10(a) displays that the disorder Δ_3 develops as the energy scale is lowered due to the dynamical-generated mechanism of disorder scatterings. However, it is of particular importance to point out that such dynamical-generated mechanism cannot be activated once two of disorders Δ_1 , Δ_2 , and Δ_3 are absent at the initial point as delineated in Fig. 10(b). In sharp contrast with disorders $\Delta_{1,2,3}$, we notice that the disorder Δ_4 shown in Fig. 10(b) cannot contribute to the dynamical-generated scenario. This means that

it does neither participate in the generation of certain disorder nor can be formed by the other sorts of disorders. Accordingly, we argue that the disorders Δ_1 , Δ_2 , and Δ_3 are closely entangled with each other but instead the disorder Δ_4 seems to be independent of other disorders. This may be rooted in the combination of the unique dispersions of nodal-line fermions, and the distinguished features of disorder themselves as well as intimate interplay with fermion-fermion interactions.

In addition, we assume all of four sorts of disorders are present and shed light on the low-energy fates of disorders under the close competition among themselves with the variations of initial conditions. One can clearly infer from Fig. 10(c) that the disorders Δ_1 and Δ_2 together with Δ_3 quickly climb up via lowering the energy scale and go toward divergence as approaching the critical scale at $l = l_c$ (the basic results for Δ_2 and Δ_3 are similar). Conversely, the strength of disorder Δ_4 is gradually diminished and eventually vanishes at the lowest-energy limit. On the one side, this signals that the disorder Δ_4 is unsusceptible to the interplay among disorders and thus indeed shares the analogous low-energy properties with the circumstance where it presents alone as shown in Fig. 7, which is in well consistent with the basic conclusion in the previous paragraph. On the other side, the tendencies of both the disorders Δ_2 and Δ_3 , which are driven to vanish if only one of them is present, are heavily reshaped by the competition among disorders.

Last but not the least important, it is necessary to address several comments on the critical energy scale represented by l_c in the presence of all types of disorders. After paralleling the similar numerical analysis, we find that initial values of fermion-fermion interactions as behaved for the presence of sole type of disorder nearly do not influence the critical energy scale. In sharp contrast, the bigger initial strengths are in favor of supporting the increase in disorders and make the critical energy scale a little bigger causing the instability to occur in advance, which is also analogous to its sole-disorder counterpart illustrated in Fig. 7. As for the beginning anisotropy of fermion velocities, it bears strong similarities to the single type of disorder displayed in Fig. 8 as well. One can notice that the strong anisotropy where v_{z0}/v_{p0} is taken as either a big or small value is preferable to hamper the divergence of disorder. However, there exists certain moderate anisotropy with $v_{z0}/v_{p0} \approx 0.1$ tends to facilitate the increase of disorder strength with the considerably bigger critical energy scales.

Before moving further, we would like to give a short summary for the low-energy fates of all kinds of disorders. As schematically summarized in Fig. 11, we find that certain dynamical-generated disorder can be generated owing to the disorder competitions which are primarily involved the interplay of disorders Δ_1 , Δ_2 , and Δ_3 but not the disorder Δ_4 . Compared to the sole presence of disorder in Sec. V A 1, the fates of Δ_2 plus Δ_3

influenced by the disorder competitions are qualitatively reformulated from vanishment to divergence in the low-energy regime and conversely for the Δ_4 , but instead the Δ_1 's is not changed. It is noteworthy that the divergence of disorder may point to a disorder-dominated diffusive metallic state [48, 71–76]. Regarding the initial conditions, both beginning values of disorder strengths and anisotropy of fermion velocities bring out the substantial impacts on the low-energy behaviors whereas the effects of starting fermion-fermion interactions are negligible.

B. Fates of fermion-fermion interactions

With the low-energy fates of the disorders in hand, we are, therefore, suitable to consider and reveal the interesting properties of fermion-fermion interactions.

1. Single type of disorder

At first, we take into account the presence of only one type of disorder and defer the general multiple types of disorders to the subsequent Sec. VB 2.

To this end, let us assume only one of disorder equations exists and participates in the coupled equations (20)-(33). After carrying out the numerical calculations and comparing them with the clean-limit behaviors of fermion-fermion interactions shown in Sec. IV A, we realize that the low-energy tendencies of fermion-fermion interactions are considerably dependent upon concrete kind of disorder. Specifically, the tendencies of fermion-fermion interactions cannot be altered by the sole presence of disorder Δ_4 as depicted in Fig. 12 compared to their clean-limit counterparts. But rather, Figs. 13-15 indicate that the presence of any one of Δ_1 , Δ_2 , or Δ_3 can be capable of dramatically changing the fates of fermion-fermion interactions. Colloquially, the fermion-fermion interactions are driven to be divergent at the critical energy l_c by the contributions from disorder scattering, which may cause certain instability and make the system unstable.

In principle, these results are in well consistent with the behaviors of disorders in Sec. VA and fermion velocities in Sec. VC, which in other words, inherit from both the fates of disorders and fermion velocities. As to the disorder Δ_1 , its unique low-energy behaviors presented in Sec. VA make a profound effect to the fermion-fermion interactions. Learning from Fig. 13(a), the sole presence of Δ_1 completely hinders the decrease in fermionic couplings at clean limit case and makes them climb up quickly, which goes toward divergence at certain critical energy scale denoted by l_c . Additionally, one can notice from Fig. 13(b) and Fig. 13(c) that this basic result is insusceptible to the starting conditions of

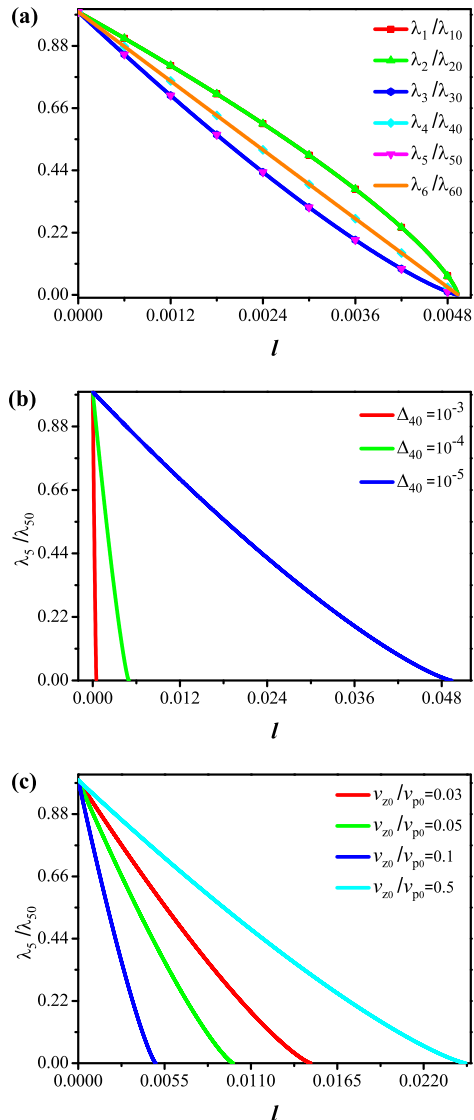


FIG. 12. (Color online) Energy-dependent evolutions of (a) λ_i/λ_{i0} ($i = 1 - 6$) with $v_{z0}/v_{p0} = 0.1$, $\lambda_0 = 10^{-4}$ and $\Delta_{40} = 10^{-4}$; (b) λ_5/λ_{50} at $\lambda_0 = 10^{-4}$ and $v_{z0}/v_{p0} = 0.1$ with several representative values of initial strengths of Δ_4 ; and (c) λ_5/λ_{50} at $\Delta_{40} = 10^{-4}$ with different initial values of anisotropy v_{z0}/v_{p0} .

all interaction parameters which are prone to modifying the critical scale l_c with a bigger Δ_{10} and a moderate v_{z0}/v_{p0} corresponding to a smaller l_c . In comparison, although the sole presence of Δ_4 shares the similar behaviors with Δ_1 as shown in Sec. VA, Fig. 12 suggests that it contributes negligibly to the fermion-fermion interactions. In particular, such result is insensitive to the initial values of other parameters as shown in Fig. 12(b) and Fig. 12(c). Several analytical comments are necessary to clarify this point. Taking the λ_6 for instance

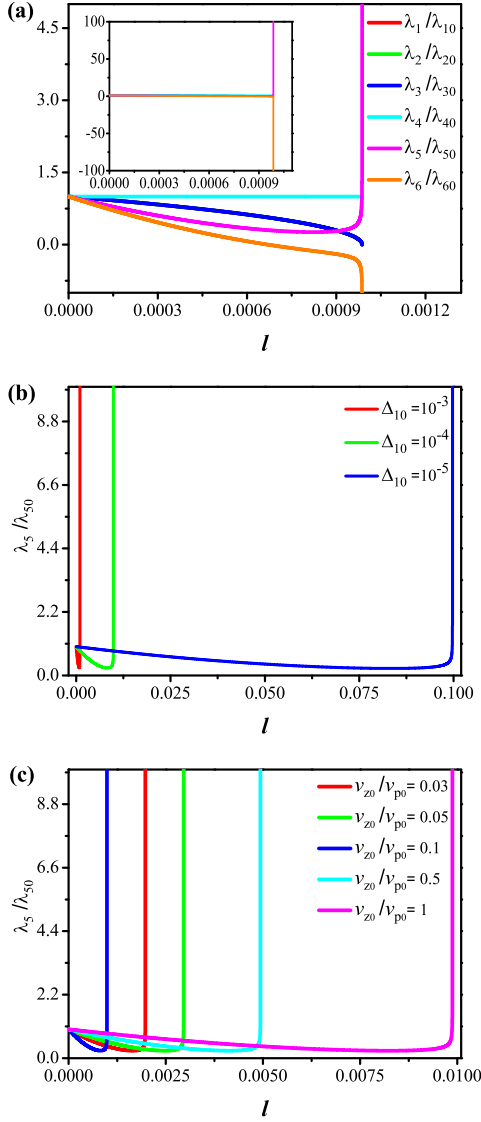


FIG. 13. (Color online) Energy-dependent evolutions of (a) λ_i/λ_{i0} ($i = 1 - 6$) with $v_{z0}/v_{p0} = 0.1$, $\lambda_0 = 10^{-3}$ and $\Delta_{10} = 10^{-3}$; (b) λ_5/λ_{50} at $\lambda_0 = 10^{-3}$ and $v_{z0}/v_{p0} = 0.1$ with several representative values of initial strengths of Δ_1 ; and (c) λ_5/λ_{50} at $\Delta_{10} = 10^{-3}$ with different initial values of anisotropy v_{z0}/v_{p0} .

(other fermion-fermion interactions are analogous), its RG equation (27) with the equal initial values at clean limit reads

$$\frac{d\lambda_6}{dl} = 2\lambda_6 \left[-\frac{1}{2} + \mathcal{C}_1(-\lambda_5 - 3\lambda_6) - (\mathcal{C}_3\lambda_2 + \mathcal{C}_4\lambda_1) \right] + 2\mathcal{C}_1\lambda_2\lambda_5. \quad (41)$$

Based on the definitions of coefficients \mathcal{C}_i in Eqs. (34)-(40), one can figure out that the first (term1) and second

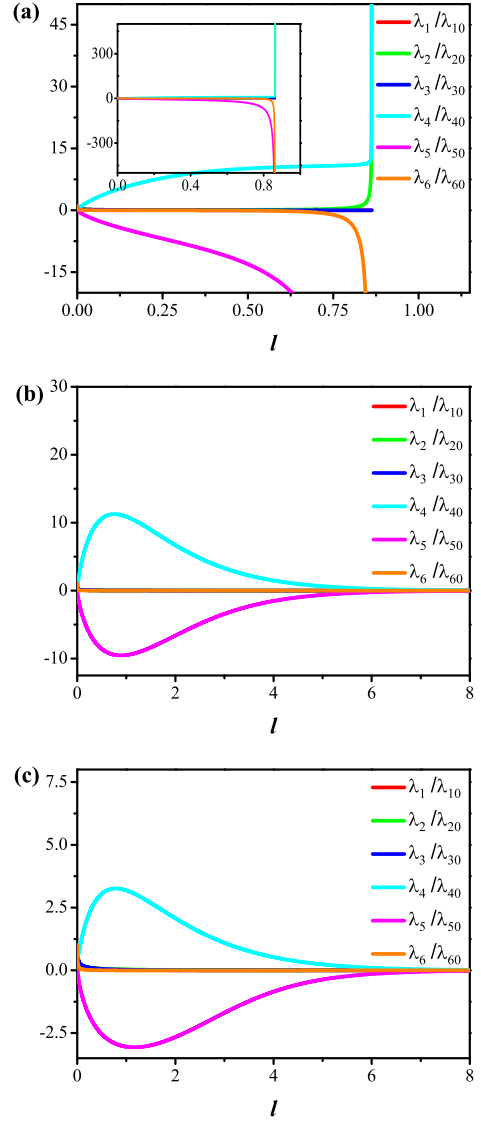


FIG. 14. (Color online) Energy-dependent evolutions of fermion-fermion couplings under different initial conditions: (a) $v_{z0}/v_{p0} = 0.1$, $\lambda_{i0} = 10^{-3}$ and $\Delta_{20} = 10^{-3}$; (b) $v_{z0}/v_{p0} = 0.1$, $\lambda_{i0} = 10^{-4}$, $\Delta_{20} = 10^{-3}$; and (c) $v_{z0}/v_{p0} = 0.5$, $\lambda_{i0} = 10^{-3}$ and $\Delta_{20} = 10^{-3}$.

(term2) terms of right hand side (RHS) of Eq. (41) satisfy $\text{term1} < 0$ and $\text{term2} > 0$ with $|\text{term2}| < |\text{term1}|$, which implies that $\frac{d\lambda_6}{dl} < 0$ and hence λ_6 decreases and tends toward zero at the lowest-energy limit. Switching on Δ_4 , its RG equation is henceforth reformulated as

$$\frac{d\lambda_6}{dl} = 2\lambda_6 \left[-\frac{1}{2} + \mathcal{C}_1(-\lambda_5 - 3\lambda_6) - (\mathcal{C}_3\lambda_2 + \mathcal{C}_4\lambda_1) - \mathcal{C}_2(\Delta_{41} + \Delta_{42}) \right] + 2\mathcal{C}_1\lambda_2\lambda_5. \quad (42)$$

This suggests that the disorder-contributed term is neg-

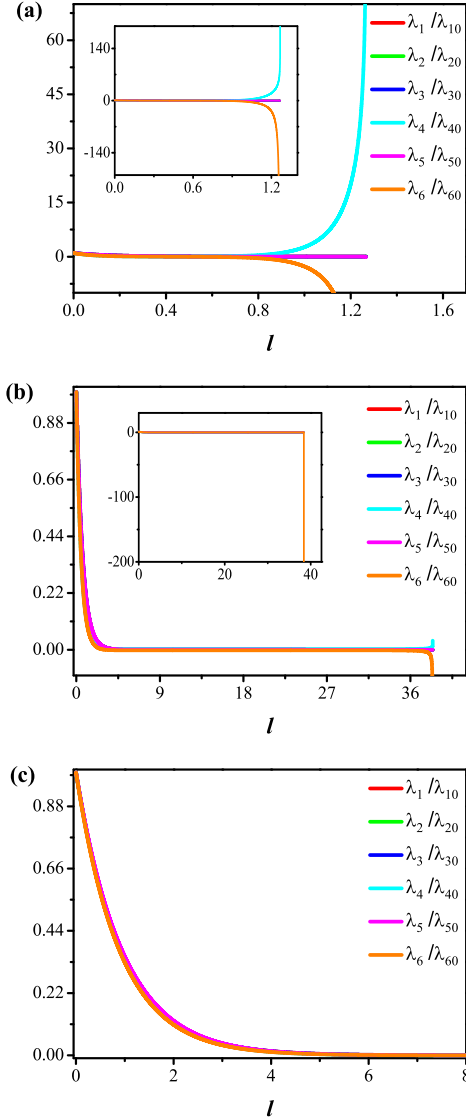


FIG. 15. (Color online) Energy-dependent evolutions of fermion-fermion couplings for anisotropy $v_{z0}/v_{p0} = 0.1$ and fermion interaction $\lambda_{i0} = 10^{-4}$ with different initial strengths of disorder Δ_{30} : (a) $\Delta_{30} = 10^{-5}$, (b) $\Delta_{30} = 10^{-6}$, and (c) $\Delta_{30} = 10^{-7}$.

ative, and thus the disorder term is helpful to decrease the λ_6 as also displayed in Fig. 12(b) that the larger initial value of Δ_4 corresponds to the faster decrease of the fermionic interaction.

Then, we move to the disorder Δ_2 or Δ_3 . With respect to these two kinds of disorders that are unimportant in the low-energy regime for themselves as shown in Sec. V A, it is of particular importance to point out that they behave like certain catalyst to arouse and ignite the fermion-fermion interactions to exhibit the distinct fates compared to clean limit's as displayed in Figs. 14-15.

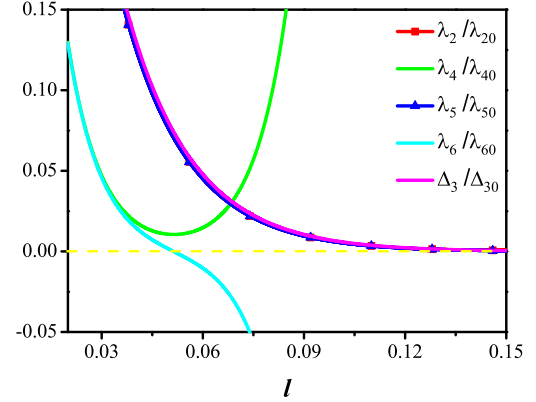


FIG. 16. (Color online) Part region for energy-dependent flows for λ_6 in the sole presence of Δ_3 at $v_{z0}/v_{p0} = 0.1$, $\lambda_0 = 10^{-4}$, and $\Delta_{30} = 10^{-4}$.

For the Δ_3 , Fig. 15 indicates that the fate of fermionic couplings can be altered as long as the Δ_{30} is suitable. In other words, the initial value of Δ_3 takes a leading responsibility and other parameters play subordinate roles. Compared to the disorder Δ_3 , the sole presence of Δ_2 cannot trigger the divergence of fermionic couplings itself. However, it is able to make them divergent under the suitable initial fermion-fermion strengths in tandem with the proper anisotropy of fermion velocities ($v_{z0}/v_{p0} \approx 0.1$) that enter into the coefficients of C_i . In analogy with the analysis for the Δ_4 , these can be roughly understood as follows. For the sake of simplicity, we only consider the λ_6 in the presence of Δ_3 whose RG equation is reduced to

$$\frac{d\lambda_6}{dl} = 2\lambda_6 \left[-\frac{1}{2} + C_1(-\lambda_5 - 3\lambda_6) - (C_3\lambda_2 + C_4\lambda_1) \right] + 2C_1\lambda_2\lambda_5 - 4C_5\lambda_4\Delta_3. \quad (43)$$

According to the evolution information in Fig. 16, the RHS of λ_6 's equation including the Δ_3 's contribution keeps negative at $l > l^*$ where l^* is defined by $\lambda_6(l^*) = 0$ once the second-line RHS of Eq. (43) ($2C_1\lambda_2\lambda_5 - 4C_5\lambda_4\Delta_3$) is less than zero. As a result, λ_6 continues to decrease and finally goes toward divergence at the critical energy scale. Paralleling above analysis for Δ_2 gives rise to the similar results.

2. Multiple types of disorders

Subsequently, let us briefly address the results for the simultaneous presence of multiple types of disorders.

Following the similar strategy in Sec. V B 1 to carry out the analogous numerical analysis of RG equations (20)-(33), we find that different types of disorders

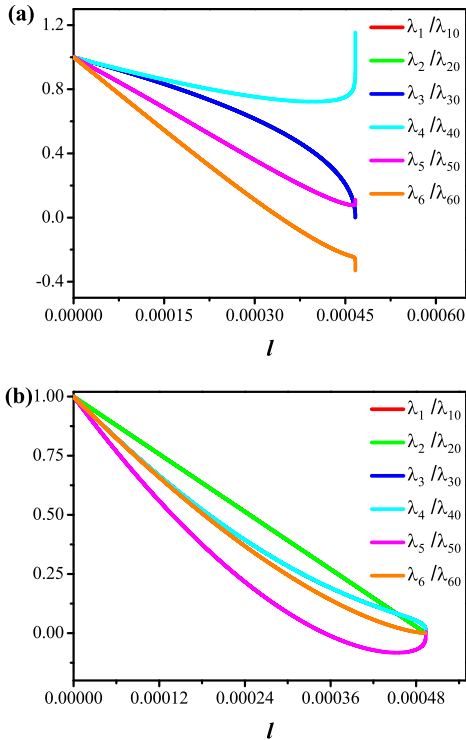


FIG. 17. (Color online) Energy-dependent evolutions of fermion-fermion couplings λ_i/λ_{i0} at $v_{z0}/v_{p0} = 0.1$ and $\lambda_{i0} = 10^{-3}$ with $i = 1 - 6$ for (a) $\Delta_{1,3} = 10^{-3}$ and (b) $\Delta_{2,4} = 10^{-3}$.

would intimately entangle and compete with each other. Such ferocious competition among distinct sorts of disorders prefers to render only two kinds of scenarios for the low-energy behaviors of fermion-fermion couplings, which are in sharp contrast with their counterparts in the sole presence of disorder.

On the one hand, the fermion-fermion couplings are prone to flowing toward certain finite values as delineated in Fig. 17(a) where Δ_1 and Δ_3 are present initially. It is worth stressing that the basic conclusion of Fig. 17(a) is always stable as long as the disorder Δ_1 exists no matter it presents at the starting point or is generated by other types of disorders as investigated in Sec. V A 2 (the corresponding results are analogous and hence not shown hereby for simplicity). As a consequence, this also supports that the disorder Δ_1 plays a more important role in the competition among other types of disorders, which is in well agreement with our analysis in Sec. V A. On the other hand, the fermion-fermion strengths λ_i with $i = 1 - 6$ gradually decrease and eventually vanish at the low-energy limit once the disorder Δ_1 is absent in the competition as displayed in Fig. 17(b) for taking the existence of Δ_2 and Δ_4 as an example.

To be brief, distinct types of disorders together with

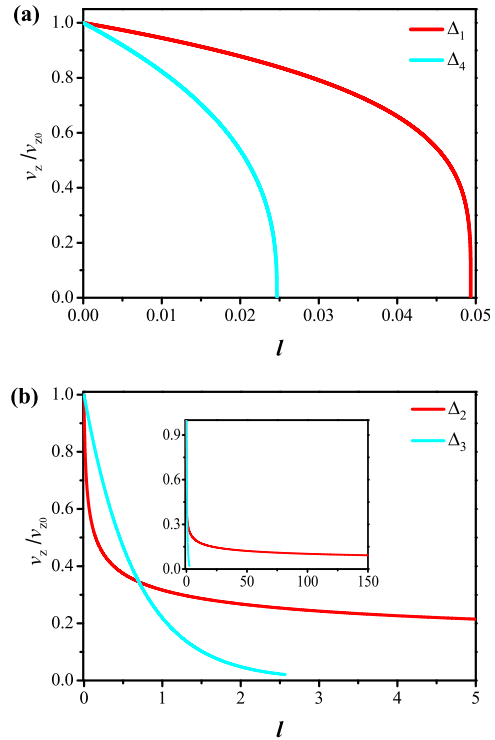


FIG. 18. (Color online) Energy-dependent evolutions of v_z/v_{z0} in the presence of disorder (a) Δ_1 or Δ_4 with $v_{z0}/v_{p0} = 0.5$ and (b) Δ_2 or Δ_3 with $v_{z0}/v_{p0} = 0.1$ at $\lambda_0 = 10^{-4}$, $\Delta_0 = 10^{-4}$ (the qualitative results are insensitive to the initial values of interaction parameters).

their unique furious competition yield different fates of fermion-fermion couplings in the low-energy. Concretely, the disorder Δ_1 takes in charge the dominant contribution and disorders $\Delta_{2,3}$'s effects are subordinate to Δ_1 's but rather the disorder Δ_4 provides a negligible impact.

C. Behaviors of fermion velocities

Furthermore, armed with the energy-dependent properties of disorders and fermion-fermion couplings, we subsequently move to study how the fermion velocities behave with lowering the energy scale in the presence of disorders.

As addressed in Sec. IV B, the fermion-fermion interactions are helpful to increase the fermion velocities. In comparison, the disorders are prone to reducing them after learning from Eq. (20) and Eq. (21). Principally, the energy-dependent coupled RG equations (20)-(33) codify the intimate competition between disorder scatterings and fermionic interactions. In order to investigate the final fates of fermion velocities under the competi-

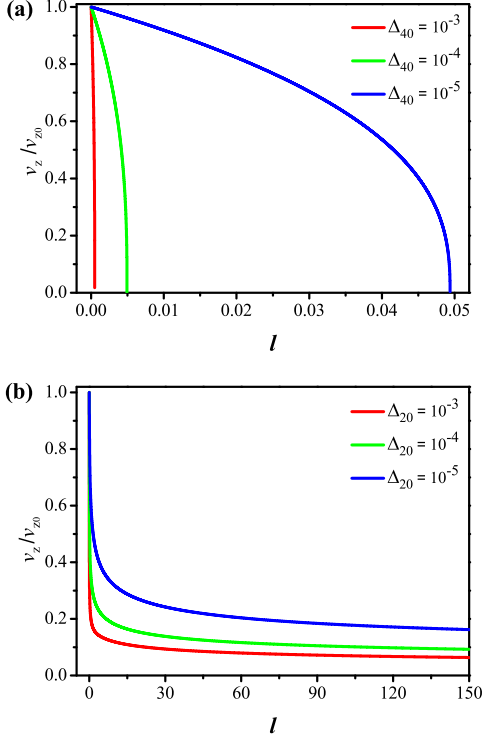


FIG. 19. (Color online) Energy-dependent evolutions of v_z/v_{z0} with several representative values of initial disorder strengths at $v_{z0}/v_{p0} = 0.1$ and $\lambda_0 = 10^{-4}$ for the presence of disorder (a) Δ_4 and (b) Δ_2 , respectively.

tion between disorder scatterings and fermionic interactions, we perform the numerical analysis and present our main results in Figs. 18-22, which indicate that disorders win the competition and hence dominate the tendencies of fermion velocities in the low-energy regime.

To be concrete, we find that v_z and v_p gradually decrease upon lowering the energy scale and their final fates heavily hinge upon the disorders. For convenience, we at first inspect the energy-dependent evolution of v_z in details and then briefly examine the ratio v_z/v_p from which the behavior of v_p can be extracted. Inheriting from Sec. V A, different types of disorders own distinct fates and, as a result, correspond to distinct sorts of evolutions depicted in Figs. 18-21.

Considering several representative groups of initial conditions, one can read from Fig. 18(a) that v_z clearly decreases and goes toward zero in the sole presence of Δ_1 or Δ_4 due to the divergence of disorder strength. It is interesting to notice that Δ_4 is more harmful to v_z than Δ_1 , which implies that v_z vanishes at some higher energy scale if there only exists Δ_4 . In marked contrast, Fig. 18(b) suggests that v_z quickly decreases and is eventually driven to certain finite value when only Δ_2 or Δ_3 is present. Compared to Δ_3 , v_z with sole presence of Δ_2

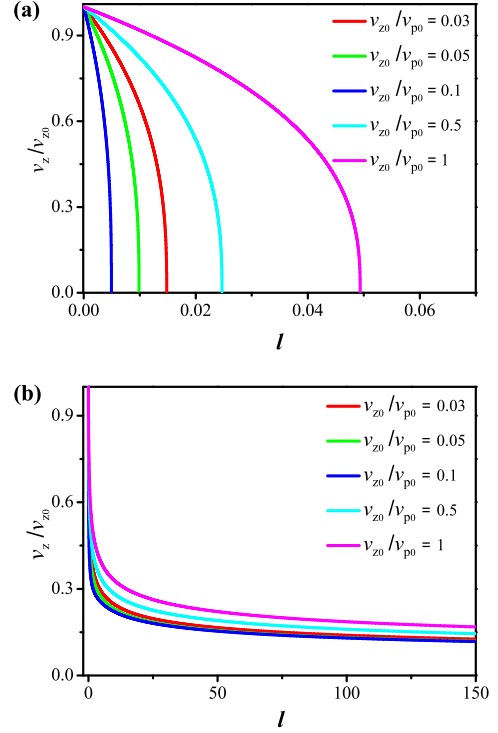


FIG. 20. (Color online) Energy-dependent evolutions of v_z/v_{z0} under several representative groups of initial anisotropy v_{z0}/v_{p0} for the presence of disorder (a) Δ_4 with $\Delta_{40} = 10^{-4}$, $\lambda_0 = 10^{-4}$, and (b) Δ_2 with $\Delta_{20} = 10^{-4}$ and $\lambda_0 = 10^{-3}$, respectively.

features a bigger critical value which is linked to a much lower critical energy scale. In order to further elucidate this point, we deliver some coarse comments on the v_z at the lowest-energy limit. Concerning the presence of disorder Δ_2 for an instance, the energy-dependent equation of v_z (20) reduces to $dv_z/dl = -C_2\Delta_2v_z$. As presented in Sec. V A, Δ_2 finally vanishes at the lowest-energy limit and, accordingly, v_z is saturated at certain nonzero value once one assumes all other parameters to be energy-independent.

Besides these qualitative conclusions, Figs. 19-21 illustrate the quantitative contributions from the distinct starting conditions. With variations of the initial values of disorders, Fig. 19 shows that the bigger initial strengths lift up the critical energy scale a little and are in favor of the decrease in fermion velocities. Fig. 20 exhibits that there exists a moderate anisotropy with $v_{z0}/v_{p0} \approx 0.1$ to facilitate the decrease in fermion velocities but instead the strong anisotropy of fermion velocities is preferable to hamper the drop of v_z or v_p . Particularly, the initial values of fermion-fermion interactions play an important role as well. We can learn from Fig. 21(a) for the presence of Δ_2 that the bigger

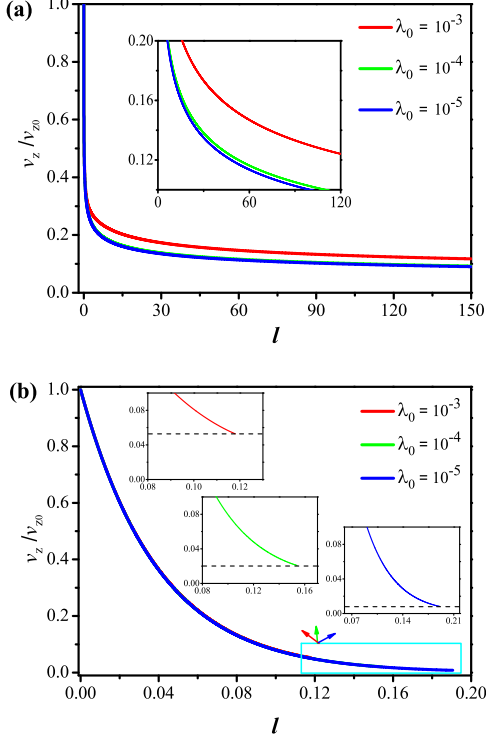


FIG. 21. (Color online) Energy-dependent evolutions of v_z/v_{z0} under several representative groups of initial fermion-fermion couplings at $v_{z0}/v_{p0} = 0.1$ for the presence of disorder (a) Δ_2 with $\Delta_{20} = 10^{-4}$ and (b) Δ_3 with $\Delta_{30} = 10^{-4}$, respectively.

initial strengths of fermionic interactions inhibit the decrease in fermion velocities. Fig. 21(b) shows that the saturated values of fermion velocities are slightly modified in the sole presence of Δ_3 . Before moving further, it is of necessity to briefly address that the basic results for the presence of more than one sorts of disorders bear similarities to the conclusions for the sole type of disorder presented above and henceforth are not shown for brevity. Colloquially, v_z decreases and is eventually driven to zero as long as the disorders dominate over the fermionic couplings and become divergent in the low-energy regime. Otherwise, it goes toward some finite value.

In addition to the behavior of v_z , let us investigate the evolution of the anisotropy of fermion velocities v_z/v_p , from which the information of v_p can be derived together with v_z 's tendencies. Generally, its low-energy tendency clusters into two distinct scenarios. On the one side, while the fermion-fermion interactions are subordinate to the disorder contribution and become less and less important with lowering the energy scale, the ratio v_z/v_p is preferable to hardly fluctuate and nearly keep invariant, which are concomitant to the clean-limit

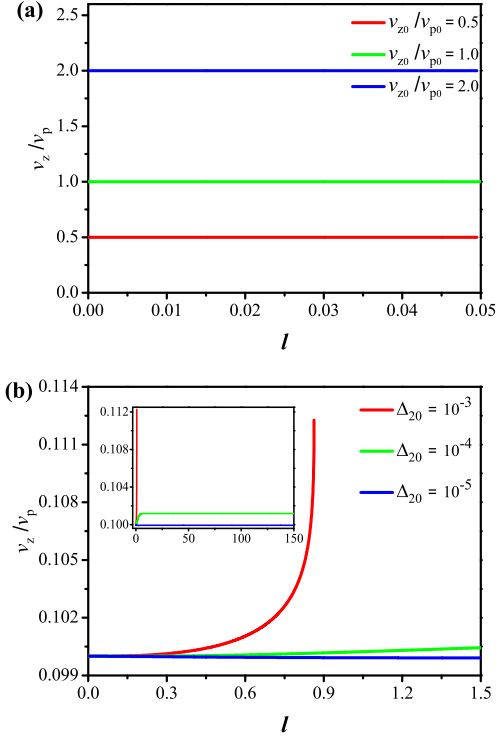


FIG. 22. (Color online) Energy-dependent evolutions of anisotropy v_z/v_p under the presence of disorder (a) Δ_1 with several representative values of v_{z0}/v_{p0} at $\lambda_0 = 10^{-3}$ and $\Delta_{10} = 10^{-4}$ (the basic results are insensitive to the concrete values of Δ_{10}), and (b) Δ_2 with several representative values of initial strengths of Δ_{20} at $v_{z0}/v_{p0} = 0.1$ and $\lambda_0 = 10^{-3}$, respectively.

case contributed by the irrelevant fermion-fermion interactions in Sec. IV B. Taking the sole presence of Δ_1 for instance, we find from Fig. 22(a) that the ratio of fermion velocities is baldly insusceptible to the variation of energy scales regardless of both the starting ratio and disorder strength. In other words, v_z shares the similar energy-dependent evolutions with v_p in this situation. On the other side, once the disorder strength is irrelevant and rapidly vanishes via lowering the energy scale, the fermion-fermion interaction is expected to play a more significant role. In such circumstance, the v_z would obtain much more supports than v_p , evincing that the anisotropy of fermion velocity deviates largely from isotropy. As illustrated in Fig. 22(b), we notice that the ratio of fermion velocities roughly gets a 12 percent increase with suitable initial conditions. Again, we stress that the qualitative conclusions are analogous for the presences of more than one sorts of disorders. To be brief, Fig. 23 catalogs our primary conclusions for the low-energy fates of fermion velocities under the competition between fermionic interactions and disorder

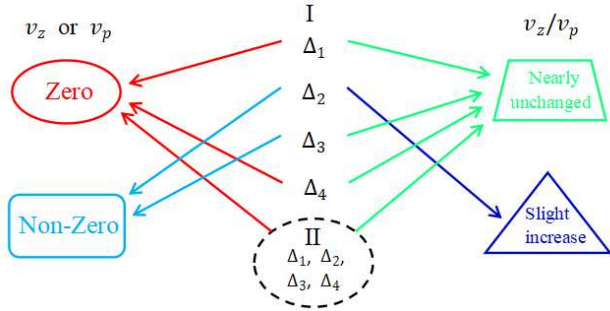


FIG. 23. (Color online) Schematic diagrams present the primary results of fermion velocities and their ratio. Hereby, the accompanied arrows point to the final fates of related quantities at the lowest-energy limit. In addition, the areas I and II correspond to the presence of only one type of disorder and multiple types of disorders, respectively.

scatterings.

VI. Summary

In summary, we utilize the powerful momentum-shell RG approach [67–69] to unbiasedly investigate the low-energy physical consequences generated by short-ranged fermion-fermion interactions and disorder scatterings as well as their competitions in the 3D line-nodal superconductors. The coupled RG evolutions of both fermion-fermion and fermion-impurity strengths that contain the low-energy physics are derived via practicing the standard RG analysis on the basis of one-loop corrections. Performing the numerical analysis of these coupled RG equations indicates that disorder strengths and fermion-fermion interactions as well as fermion velocities exhibit a number of interesting properties in the low-energy regime.

For the sake of completeness, we commence with the clean-limit circumstance. In such a situation, the fermion-fermion interactions are forced to decrease and finally vanish with lowering the energy scale. This causes that fermion velocities $v_{z,p}$ increase in the beginning and finally flow toward some saturated constants. Meanwhile, the anisotropy of fermion velocities v_z/v_p can be also revised under the contributions from fermion-fermion interactions. With the initial conditions $v_{z0}/v_{p0} < 1$ and $v_{z0}/v_{p0} > 1$, it would receive a slight decrease and increase, respectively. Subsequently, we put our focus on the consequences of competitions between fermion-fermion couplings and disorder scatterings. At the outset, we assume that there only exists a single type of disorder and find that the disorder strength monotonously decreases for $\Delta_{2,3}$ and goes toward divergence for $\Delta_{1,4}$ with lowering the energy scale, respectively. In particular, the relevant disorder

may result in a disorder-dominated diffusive metallic state [48, 71–76]. With respect to the presence of multiple types of disorders, we figure out that only Δ_1 holds its sole-presence property and remains relevant. In sharp contrast, the fates of other three types of disorders are sensitive to the competitions among distinct types of disorders. On the one hand, the Δ_4 can be driven to be irrelevant but instead Δ_2 and Δ_3 being changed to be divergent. On the other hand, certain dynamical-generated disorder which is absent initially can be induced due to the disorder competitions once two sorts of disorders Δ_1 , Δ_2 , and Δ_3 are present at the starting point. Then, the effects of disorders on fermion-fermion couplings are addressed. The sole presence of Δ_1 (Δ_2 or Δ_3) is of particular importance to increase the fermion-fermion interactions and even drive them toward divergence at certain critical energies although the disorder Δ_4 provides a negligible impact. However, the intimate competition among distinct types of disorders can weaken and neutralize the disorder contributions, which accordingly causes the fermionic couplings to evolve toward zero or certain finite nonzero values. Further, we briefly deliver the behaviors of fermion velocities under the interplay between fermion-fermion interactions and disorders. For the sole presence of Δ_1 (or Δ_4) or multiple kinds of disorders, the fermion velocities progressively decrease and vanish at the lowest-energy limit but instead they are attracted by some certain saturated value for the single presence of Δ_2 (or Δ_3). Additionally, the ratio v_z/v_p would receive a little increase while the fermion-fermion interactions dominate over the disorders. In comparison, it nearly keeps invariant once the latter wins the former in the low-energy regime. For convenience, we employ Fig. 11 in conjunction with Fig. 23 to schematically present our central conclusions.

In principle, the interaction and disorder-induced signatures are closely associated with the fixed points of systems in the parameter space and henceforth the potential instabilities as well as phase transitions. As a corollary, the properties of physical quantities around the fixed points may be altered and modified, and, accordingly, such unusual signatures may be indirectly probed by detecting the physical quantities including the density of states, spectral function, specific heat, etc., which are expected to inherit parts of information from the disorder-induced instabilities [100]. Lastly, we hope that our results would provide helpful clues for further experiments to examine the low-energy behaviors of physical implications that are associated with fermion velocities and phase transitions in the 3D nodal-line superconductors.

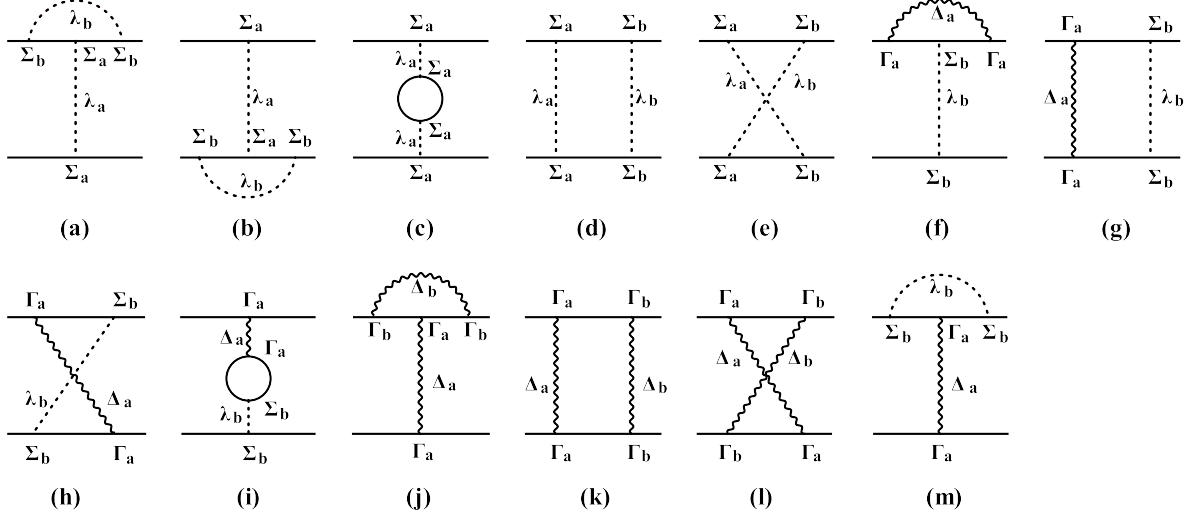


FIG. 25. One-loop corrections to the fermion-fermion couplings (a)-(i) and the fermion-disorder strengths (j)-(m) (the solid, dashed and wavy lines represent the fermion propagator, fermion-fermion interactions, and disorder scattering, respectively) [57, 70].

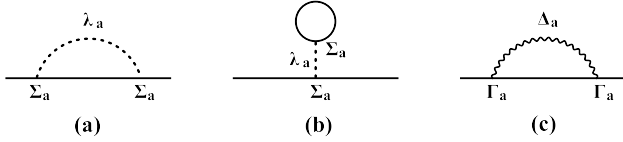


FIG. 24. One-loop corrections to the fermion propagator due to the fermion-fermion interactions (a) and (b) as well as disorder scatterings (c) (the solid, dashed, and wavy lines represent the fermion propagator, fermion-fermion interaction, and disorder scattering, respectively).

ACKNOWLEDGEMENTS

W.H.B. thanks Dr. Wen Liu and M.S. Xiao-Yue Ren for the helpful discussions. J.W. was partially supported

by the National Natural Science Foundation of China under Grant No. 11504360.

A. One-loop corrections

To be convenient, we collect all the one-loop corrections within this appendix. Starting from our effective theory (12), the fermionic propagator as well as fermion-fermion couplings and fermion-disorder strengths would receive the one-loop corrections due to their intimate interplays as diagrammatically exhibited in Fig. 24 and Fig. 25, respectively. After performing tedious but straightforward calculations [32, 33, 38, 45], we obtain

$$\Sigma(i\omega, \mathbf{k}) = \int \frac{d^3\mathbf{k}d\omega}{(2\pi)^4} \psi_{\mathbf{k},\omega}^\dagger \{ [C_2(\Delta_1 + \Delta_2 + \Delta_3 + \Delta_{41} + \Delta_{42} + \Delta_{43})l](i\omega) - (4C_1\lambda_2l)v_z\delta k_z\Sigma_{03} - (4C_1\lambda_1l)v_p\delta k_\perp\Sigma_{01} \} \psi_{\mathbf{k},\omega}, \quad (\text{A1})$$

for the one-loop corrections to the noninteracting fermionic propagator. In addition, the fermion-fermion couplings appearing in Eq. (9) would receive the one-loop corrections from Fig. 25 as follows

$$\delta\lambda_1 = \lambda_1 [2C_3(-3\lambda_1 - 2\lambda_2 - \lambda_3 + \lambda_4 + \lambda_5 - \lambda_6) + 2C_7(\Delta_1 - \Delta_2 + \Delta_3 - \Delta_{41} - \Delta_{42} - \Delta_{43} - 8\Delta_3)]l, \quad (\text{A2})$$

$$\delta\lambda_2 = \lambda_2 [2C_4(-2\lambda_1 - 3\lambda_2 + \lambda_3 + \lambda_4 - \lambda_5 - \lambda_6) + 2C_7(-\Delta_1 + \Delta_2 + \Delta_3 - \Delta_{41} - \Delta_{42} - \Delta_{43})]l, \quad (\text{A3})$$

$$\delta\lambda_3 = \{ \lambda_3 [2C_4(-2\lambda_1 + \lambda_2 - 3\lambda_3 - \lambda_4 + \lambda_5 + \lambda_6) + 2C_7(\Delta_2 - \Delta_1 + \Delta_3 + \Delta_{41} + 7\Delta_{42} + \Delta_{43})] - 4C_6\lambda_5\Delta_{41} \} l \quad (\text{A4})$$

$$\delta\lambda_4 = [2\lambda_4(C_2\Delta_1 + C_2\Delta_2 + C_2\Delta_3 - C_2\Delta_{41} - C_2\Delta_{42} + C_2\Delta_{43}) - 2(2C_5\lambda_5\Delta_2 + 2C_5\lambda_6\Delta_3 + C_4\lambda_2\lambda_6 + C_3\lambda_1\lambda_6)]l \quad (\text{A5})$$

$$\delta\lambda_5 = \{ \lambda_5 [2C_3(\lambda_1 - 2\lambda_2 + \lambda_3 + \lambda_4 - 3\lambda_5 - \lambda_6) + 2(C_7\Delta_1 - C_7\Delta_2 + C_7\Delta_3 + C_7\Delta_{41} + C_7\Delta_{42} - C_7\Delta_{43})] + 2C_1\lambda_2\lambda_6 - 4(C_6\lambda_3\Delta_{41} + C_5\lambda_4\Delta_2 + C_5\lambda_6\Delta_1) \} l, \quad (\text{A6})$$

$$\delta\lambda_6 = \{ \lambda_6 [2C_1(-\lambda_1 - \lambda_2 + \lambda_3 + \lambda_4 - \lambda_5 - 3\lambda_6) - 2(C_3\lambda_2 + C_4\lambda_1) + 2(-C_2\Delta_1 - C_2\Delta_2 + C_2\Delta_3$$

$$-C_2\Delta_{41} - C_2\Delta_{42} + C_2\Delta_{43})] + 2C_1\lambda_2\lambda_5 - 4C_5(\lambda_4\Delta_3 + \lambda_5\Delta_1)]l. \quad (\text{A7})$$

Furthermore, the one-loop corrections from Fig. 25 contributing to the disorder scatterings involved in Eq. (11) take the form of [39, 40]

$$\delta\Delta_1 = \{\Delta_1[4C_2(\Delta_1 + \Delta_2 + \Delta_3 + \Delta_{41} + \Delta_{42} + \Delta_{43})] + 8C_5\Delta_2\Delta_3\}l, \quad (\text{A8})$$

$$\delta\Delta_2 = \{\Delta_2[4C_2(\Delta_3 - \Delta_1 - \Delta_2 + \Delta_{41} + \Delta_{42} + \Delta_{43}) + C_1(\lambda_1 + \lambda_2 + \lambda_3 - \lambda_4 + \lambda_5 - \lambda_6)] + 8C_5\Delta_1\Delta_3\}l, \quad (\text{A9})$$

$$\delta\Delta_3 = \{\Delta_3[4C_7(\Delta_1 - \Delta_2 + \Delta_3 - \Delta_{41} - \Delta_{42} - \Delta_{43}) + C_3(\lambda_2 - \lambda_1 + \lambda_3 - \lambda_4 - \lambda_5 + \lambda_6)] + 8C_5\Delta_1\Delta_2\}l, \quad (\text{A10})$$

$$\delta\Delta_{41} = \{\Delta_{41}[4C_7(\Delta_2 - \Delta_1 + \Delta_3 - \Delta_{41} + \Delta_{42} + \Delta_{43}) + C_4(\lambda_1 - \lambda_2 + \lambda_3 + \lambda_4 - \lambda_5 - \lambda_6)] + 8C_5\Delta_{42}\Delta_{43}\}l \quad (\text{A11})$$

$$\delta\Delta_{42} = \{\Delta_{42}[4C_7(\Delta_2 - \Delta_1 + \Delta_3 + \Delta_{41} - \Delta_{42} + \Delta_{43}) + C_4(\lambda_1 - \lambda_2 - \lambda_3 + \lambda_4 - \lambda_5 - \lambda_6)] + 8C_5\Delta_{41}\Delta_{43}\}l \quad (\text{A12})$$

$$\delta\Delta_{43} = \{\Delta_{43}[4C_7(\Delta_2 - \Delta_1 + \Delta_3 + \Delta_{41} + \Delta_{42} - \Delta_{43}) + C_4(\lambda_1 - \lambda_2 + \lambda_3 - \lambda_4 + \lambda_5 + \lambda_6)] + 8C_5\Delta_{41}\Delta_{42}\}l \quad (\text{A13})$$

where the coefficients C_i with $i = 1 - 7$ in above results (A1)-(A13) have already been designated in Eqs. (34)-(40).

-
- [1] J. Barnzsn, L. N. Cooper, and J. R. Schrieffer, *Phys. Rev.* **108**, 1175 (1957).
- [2] M. Tinkham, *Introduction to Superconductivity*, *Dover Books on Physics Series*, Dover Publications, (1996).
- [3] P. W. Anderson, *The Theory of Superconductivity in the High-Tc Cuprate Superconductors*, Princeton University Press, (1997).
- [4] A. Larkin and A. Varlamov, *Theory of fluctuations in superconductors*, Oxford University Press (New York), (2005).
- [5] P. A. Lee, N. Nagaosa, and X. -G. Wen, *Rev. Mod. Phys.* **78**, 17 (2006).
- [6] V. L. Berezinskii, *Sov. Phys. JETP* **61**, 1144 (1971).
- [7] J. M. Kosterlitz and D. J. Thouless, *J. Phys. C* **6**, 1181 (1973).
- [8] H. Ding, T. Yokoya, J. Campuzano, T. T. Takahashi, M. Randeria, M. Norman, T. Mochiku, and J. Giapintzakis, *Nature (London)*, **382**, 51 (1996).
- [9] A. G. Loeser, Z. -X. Shen, D. Desau, D. Marshall, C. Park, P. Fournier, and A. Kapitulnik, *Science* **273**, 325 (1996).
- [10] T. Valla, A. Fedorov, P. Johnson, B. Wells, S. Hulbert, Q. Li, G. Gu, and N. Koshizuka, *Science* **285**, 2110 (1999).
- [11] T. Yoshida, X. J. Zhou, T. Sasagawa, W. L. Yang, P. V. Bogdanov, A. Lanzara, Z. Hussain, T. Mizokawa, A. Fujimori, H. Eisaki, Z. -X. Shen, T. Kakeshita, and S. Uchida, *Phys. Rev. Lett.* **91**, 027001 (2003).
- [12] F. Ronning, T. Sasagawa, Y. Kohsaka, K. M. Shen, A. Damascelli, C. Kim, T. Yoshida, N. P. Armitage, D. H. Lu, D. L. Feng, L. L. Miller, H. Takagi, and Z. -X. Shen, *Phys. Rev. B* **67**, 165101 (2003).
- [13] I. Bonalde, W. Bramer-Escamilla, and E. Bauer, *Phys. Rev. Lett.* **94**, 207002 (2005).
- [14] K. Izawa, Y. Kasahara, Y. Matsuda, K. Behnia, T. Yasuda, R. Settai, and Y. Onuki, *Phys. Rev. Lett.* **94**, 197002 (2005).
- [15] N. Tateiwa, Y. Haga, T. D. Matsuda, S. Ikeda, T. Yasuda, T. Takeuchi, R. Settai, and Y. Onuki, *Journal of the Physical Society of Japan* **74**, 1903 (2005).
- [16] E. Slooten, T. Naka, A. Gasparini, Y. Huang, and A. De. Visser, *Phys. Rev. Lett.* **103**, 097003 (2009).
- [17] A. Gasparini, Y. Huang, N. Huy, J. Klaasse, T. Naka, E. Slooten, and A. De. Visser, *Journal of Low Temperature Physics* **161**, 134 (2010).
- [18] J. -P. Reid, M. Tanatar, X. Luo, H. Shakeripour, N. Doiron-Leyraud, N. Ni, S. Budko, P. Canfield, R. Prozorov, and L. Taillefer, *Phys. Rev. B* **82**, 064501 (2010).
- [19] M. Tanatar, J. -P. Reid, H. Shakeripour, X. Luo, N. Doiron-Leyraud, N. Ni, S. Budko, P. Canfield, R. Prozorov, and L. Taillefer, *Phys. Rev. Lett.* **104**, 067002 (2010).
- [20] C. -L. Song, Y. -L. Wang, P. Cheng, Y. -P. Jiang, W. Li, T. Zhang, Z. Li, K. He, L. Wang, and J. -F. Jia, H. -H. Hung, C. -J. Wu, X. Ma, X. Chen, Q. -K. Xue, *Science* **332**, 1410 (2011).
- [21] T. Watashige, Y. Tsutsumi, T. Hanaguri, Y. Kohsaka, S. Kasahara, A. Furusaki, M. Sigrist, C. Meingast, T. Wolf, and H. v. Lohneysen, T. Shibauchi, and Y. Matsuda, *Phys. Rev. X* **5**, 031022 (2015).
- [22] J. -P. Reid, M. Tanatar, X. Luo, H. Shakeripour, S. R. de Cotret, N. Doiron-Leyraud, J. Chang, B. Shen, H. -H. Wen, H. Kim, R. Prozorov, N. Doiron-Leyraud, and L. Taillefer, *Phys. Rev. B* **93**, 214519 (2016).
- [23] A. H. Castro Neto, F. Guinea, N. M. R. Peres, K. S. Novoselov, and A. K. Geim, *Rev. Mod. Phys.* **81**, 109 (2009).
- [24] M. Z. Hasan and C. L. Kane, *Rev. Mod. Phys.* **82**, 3045 (2010).
- [25] X. -L. Qi and S. -C. Zhang, *Rev. Mod. Phys.* **83**, 1057 (2011).
- [26] A. Altland, B. D. Simons, and M. R. Zirnbauer, *Phys. Rep.* **359**, 283 (2002).
- [27] E. Fradkin, S. A. Kivelson, M. J. Lawler, J. P. Eisenstein, and A. P. Mackenzie,

- Annu. Rev. Condens. Matter Phys. **1**, 153 (2010).
- [28] S. S. Das, S. Adam, E. H. Hwang, and E. Rossi, Rev. Mod. Phys. **83**, 407 (2011).
- [29] S. Sachdev, Quantum Phase Transitions 2nd edn, Cambridge: Cambridge University Press (2011).
- [30] V. N. Kotov, B. Uchoa, V. M. Pereira, F. Guinea, and Neto. A. H. Castro, Rev. Mod. Phys. **84**, 1067 (2012).
- [31] K. Sun, H. Yao, E. Fradkin, and S. A. Kivelson, Phys. Rev. Lett. **103**, 046811 (2009).
- [32] V. Cvetkovic, R. E. Throckmorton, and O. Vafek, Phys. Rev. B **86**, 075467 (2012).
- [33] J. M. Murray and O. Vafek, Phys. Rev. B **89**, 201110(R) (2014).
- [34] B. Dora, I. F. Herbut, and R. Moessner, Phys. Rev. B **90**, 045310 (2014).
- [35] I. F. Herbut and L. Janssen, Phys. Rev. Lett. **113**, 106401 (2014).
- [36] L. Janssen and I. F. Herbut, Phys. Rev. B **92**, 045117 (2015).
- [37] I. Boettcher and I. F. Herbut, Phys. Rev. B **93**, 205138 (2016).
- [38] J. Wang, J. Phys.: Condens. Matter **30**, 125401 (2018); Y. -M. Dong, D. -X. Zheng, and J. Wang, J. Phys.: Condens. Matter **31**, 275601 (2019); J. Wang, Eur. Phys. J. B **92**, 102 (2019).
- [39] B. Roy and M. S. Foster, Phys. Rev. X **8**, 011049 (2018).
- [40] B. Roy, R. J. Slager, and V. Juričić, Phys. Rev. X **8**, 031076 (2018).
- [41] A. A. Nersesyan, A. M. Tsvelik, and F. Wenger, Nucl. Phys. B **438**, 561 (1995).
- [42] T. Stauber, F. Guinea, and M. A. H. Vozmediano, Phys. Rev. B **71**, 041406 (2005).
- [43] J. Wang, G. -Z. Liu, and H. Kleinert, Phys. Rev. B **83**, 214503 (2011).
- [44] J. Wang, Phys. Rev. B **87**, 054511 (2013).
- [45] J. Wang, C. Ortix, J. van den Brink, and D. V. Efremov, Phys. Rev. B **96**, 201104(R) (2017).
- [46] K. S. Novoselov, A. K. Geim, S. V. Morozov, D. Jiang, M. I. Katsnelson, I. V. Grigorieva, S. V. Dubonos, and A. A. Firsov, Nature **438**, 197 (2005).
- [47] I. L. Aleiner and K. B. Efetov, Phys. Rev. Lett. **97**, 236801 (2006).
- [48] M. S. Foster and I. L. Aleiner, Phys. Rev. B **77**, 195413 (2008).
- [49] Y. -L. Lee and Y. -W. Lee, Phys. Rev. B **96**, 045115 (2017).
- [50] R. M. Nandkishore and S. A. Parameswaran, Phys. Rev. B **95**, 205106 (2017).
- [51] Y. -X. Wang and R. M. Nandkishore, Phys. Rev. B **96**, 115130 (2017).
- [52] R. Nandkishore, D. A. Huse, and S. L. Sondhi, Phys. Rev. B **89**, 245110 (2014).
- [53] Ipsita Mandal, Annals of Physics **392**, 179 (2018).
- [54] B. Roy, Phys. Rev. B **96**, 041113 (2017).
- [55] S. Sur and B. Roy, Phys. Rev. Lett. **123**, 207601 (2019).
- [56] B. Roy, V. Juricic, and S. D. Sarma, Scientific Reports **6**, 32446 (2016).
- [57] Y. M. Dong, Y. H. Zhai, D. X. Zheng, and J. Wang, Phys. Rev. B **102**, 134204 (2020).
- [58] Y. H. Zhai and J. Wang, Nucl. Phys. B **966**, 115371 (2021).
- [59] Y. Matsuda, K. Izawa, and I. Vekhter, Journal of Physics Condensed Matter **18**, R705 (2006).
- [60] M. Sigrist and K. Ueda, Rev. Mod. Phys. **63**, 239 (1991).
- [61] S. Sur and R. Nandkishore, New J. Phys. **18**, 115006 (2016).
- [62] M. Vojta, Y. Zhang, and S. Sachdev, Phys. Rev. Lett. **85**, 4940 (2000).
- [63] M. Vojta, Y. Zhang, and S. Sachdev, Phys. Rev. B **62**, 6721 (2000).
- [64] M. Vojta, Y. Zhang, and S. Sachdev, International Journal of Modern Physics B **14**, 3719 (2000).
- [65] M. Vojta, Rep. Prog. Phys. **66**, 2069 (2003).
- [66] H. v. Lohneysen, A. Rosch, M. Vojta, and P. Wolfle, Rev. Mod. Phys. **79**, 1015 (2007).
- [67] K. G. Wilson, Rev. Mod. Phys. **47** 773 (1975).
- [68] J. Polchinski, arXiv: hep-th/9210046 (1992).
- [69] R. Shankar, Rev. Mod. Phys. **66**, 129 (1994).
- [70] B. Roy and S. D. Sarma, Phys. Rev. B **94**, 115137 (2016).
- [71] E. Fradkin, Phys. Rev. B **33**, 3263 (1986).
- [72] K. Kobayashi, T. Ohtsuki, K. -I. Imura, and I. F. Herbut, Phys. Rev. Lett. **112**, 016402 (2014).
- [73] H. -H. Lai, B. Roy, and P. Goswami, arXiv: 1409.8675 (2014).
- [74] E. -G. Moon and Y. B. Kim, arXiv: 1409.0573 (2014).
- [75] P. Goswami and S. Chakravarty, Phys. Rev. Lett. **107**, 196803 (2011).
- [76] J. Wang, Phys. Lett. A **379** 1917 (2015).
- [77] S. Matsuura, P. -Y. Chang, A. P. Schnyder, and S. Ryu, New. J. Phys. **15**, 065001 (2013).
- [78] S. E. Han, G. Y. Cho, and E. G. Moon, Phys. Rev. B **95**, 094502 (2017).
- [79] P. Frigeri, D. Agterberg, A. Koga, and M. Sigrist, Phys. Rev. Lett. **92**, 097001 (2004).
- [80] P. Brydon, A. P. Schnyder, and C. Timm, Phys. Rev. B **84**, 020501 (2011).
- [81] B. Roy, P. Goswami, and J. D. Sau, Phys. Rev. B **94**, 041101(R) (2016).
- [82] B. Roy, Y. Alavirad, and J. D. Sau, Phys. Rev. Lett. **118**, 227002 (2017).
- [83] A. L. Szabó and B. Roy, Phys. Rev. B **103**, 205135 (2021).
- [84] I. F. Herbut, V. Juricic and B. Roy, Phys. Rev. B **79**, 085116 (2009).
- [85] S. Raj Panday and M. Dzero, Journal of Physics Condensed Matter **33**, 275601 (2021).
- [86] F. Evers and A. D. Mirlin, Rev. Mod. Phys. **80**, 1355 (2008).
- [87] P. Coleman, *Introduction to Many Body Physics* Cambridge University Press (2015).
- [88] S. Edwards and P. W. Anderson, J. Phys. F **5** 965 (1975).
- [89] P. A. Lee and T. V. Ramakrishnan, Rev. Mod. Phys. **57** 287 (1985).
- [90] I. V. Lerner, arXiv:cond-mat/0307471 (2003).
- [91] Y. Huh and S. Sachdev, Phys. Rev. B **78**, 064512 (2008).
- [92] E. -A. Kim, M. J. Lawler, P. Oreto, S.

- Sachdev, E. Fradkin, and S. A. Kivelson, Phys. Rev. B **77**, 184514 (2008).
- [93] J. -H. She, J. Zaanen, A. R. Bishop, and A. V. Balatsky, Phys. Rev. B **82**, 165128 (2010).
- [94] J. Wang and G. -Z. Liu, Phys. Rev. D **90**, 125015 (2014).
- [95] J. -H. She, M. J. Lawler, and E. -A. Kim, Phys. Rev. B **92**, 035112 (2015).
- [96] J. Wang and G. -Z. Liu, Phys. Rev. B **92**, 184510 (2015).
- [97] J. Wang, G. -Z. Liu, D. V. Efremov, and J. van den Brink, Phys. Rev. B **95**, 024511 (2017).
- [98] J. Wang, Supercond. Sci. Technol. **35**, 125006 (2022).
- [99] X. Y. Ren, Y. H. Zhai and J. Wang, Nucl. Phys. B **975**, 115651 (2022).
- [100] G. D. Mahan, *Many-Particle Physics, 2nd edn.* (Plenum, New York, 2000).